Physics of Fluids

Coupled Faxen relations for non-uniform slip Janus spheres

Cite as: Phys. Fluids **33**, 112003 (2021); https://doi.org/10.1063/5.0067895
Submitted: 20 August 2021 • Accepted: 09 October 2021 • Published Online: 02 November 2021

A. R. Premlata and Hsien-Hung Wei

Physics of Fluids ARTICLE scitation.org/journal/phf

Coupled Faxen relations for non-uniform slip Janus spheres

Cite as: Phys. Fluids **33**, 112003 (2021); doi: 10.1063/5.0067895
Submitted: 20 August 2021 · Accepted: 9 October 2021 ·
Published Online: 2 November 2021

View Online Export Citation CrossMark

A. R. Premlata and Hsien-Hung Wei[a)]

AFFILIATIONS

Department of Chemical Engineering, National Cheng Kung University, Tainan 701, Taiwan

[a)]Author to whom correspondence should be addressed: hhwei@mail.ncku.edu.tw

ABSTRACT

A non-uniform surface slip can cause a symmetry breaking in the geometry of an otherwise homogeneous spherical particle to give rise to an anisotropic hydrodynamic resistance to the particle. Here, we develop a more general theoretical framework capable of decoding the surface-pattern-dependent hydrodynamic features for single heterogeneous spheres having arbitrary non-uniform slip length distributions in small variations, especially for those of weakly stick–slip or slip–slip Janus spheres in either the two-faced or striped type. Utilizing the Lorentz reciprocal theorem in conjunction with surface spherical harmonic expansion, we derive a new coupled set of Faxen formulas for the hydrodynamic force and torque on a non-uniform slip sphere by expressing impacts of slip anisotropy in terms of surface dipole and quadrupole without solving detailed flow fields. Our results reveal not only how various additional forces/torques arise from surface dipole and quadrupole, but also that it is the anti-symmetric dipole responsible for distinctive force-rotation/torque-translation coupling. These features are very distinct from those of no-slip or uniform-slip particles, possibly spurring new means to characterize or sort Janus particles in microfluidic experiments. In addition, the coupled Faxen relations with surface moment contributions reported here may infer potential changes in the collective nature of hydrodynamic interactions between non-uniform slip spheres. Furthermore, the present framework can also be readily applied to heterogeneous self-propelled squirmers whose swimming velocities are sensitive to slip anisotropy.

I. INTRODUCTION

Janus particles are colloidal particles comprising more than one surface with distinct properties, showing promising uses in many applications, such as self-assembly and drug delivery.[1] They can be made using amphiphilic materials to possess both hydrophobic and hydrophilic faces.[2] They can also take the form of composite drops that can be conveniently made using the microfluidic approach.[3] Hydrodynamically, particles of this sort can be either stick–slip or slip–slip type because of slip disparity over their surfaces. For this reason, the hydrodynamic characteristics of these particles are expected to be very distinct from those of no-slip or uniform slip particles, which could be vital when one would like to manipulate or transport such particles. Slip and its non-uniformity may also be critical for the swimming of squirmers self-propelled by prescribed slip velocities on their surfaces[4–8] because their propulsions cannot be fully transmitted from the slip velocities. The situation could become more complicated for heterogeneous squirmers whose surfaces are mixed with stick and slip parts.

The present work is motivated by the need in understanding the hydrodynamics of stick–slip or slip–slip Janus particles in order to collaborate with a diversity of flow and actuation mechanisms for achieving more precise steering or manipulation of these particles in practice, for instance, under the theme of microfluidics. Here, we will focus on particles in the spherical shape. Our aim is to develop more general formulas for computing the hydrodynamic force and torque on a non-uniform slip Janus sphere in order to describe how the sphere behaves in its motion under arbitrary forcing or flow conditions.

The main characteristic difference between a non-uniform slip sphere and a no-slip/uniform slip sphere is that the hydrodynamic resistance of the former becomes anisotropic. This could lead a non-uniform slip sphere to experience a force when it undergoes rotation or to feel a torque when it is translating. If the slip pattern is axisymmetric like that of a Janus sphere, such translation-rotation coupling, which is absent for a homogenous sphere, is somewhat similar to that for a spheroid.[9] It is this reason why a stick–slip sphere in a parabolic flow field displays tumbling like what a spheroid does, as shown in numerical simulations by Trofa *et al.*[10] Previous studies on the hydrodynamics of a two-faced stick-slip Janus sphere mainly rely on solving detailed flow fields around the sphere.[9–13] However, it is generally difficult to see how a slip pattern affects the hydrodynamic force and torque on the sphere. This, thus, motivates us to search for whether there is a simpler way to obtain these quantities without having to solve detailed flow fields. Like the Faxen laws for no-slip and uniform-slip spheres,[14–16] we seek modifications of these laws for non-uniform slip spheres. However, such modifications will not be simple extensions to those of homogeneous spheres. This is due to the fact that the slip pattern may not have to be of two-faced type with an antisymmetric slip distribution like those considered in previous studies,[9–13,17] it can well be stripe-like or taking a dipolar form with a symmetric slip distribution. The hydrodynamic features of the latter can be very different from those of the former, especially when there is an imposed flow in which the features of the force and torque have to be further determined by the flow symmetry. Therefore, it is necessary to develop a more general framework not only for identifying how different slip patterns influence the hydrodynamics of a Janus sphere but also for handling the situations in arbitrary imposed flow fields, which is the main theme of this work.

It is worth mentioning that modified Faxen relations for two-faced stick-slip Janus spheres have been previously derived by Swan and Khair.[17] Their analysis is formulated using the integral representation of the Stokes flow solution in terms of multipole moment expansions. While this approach may appear general, it is not obvious how different modes of the slip pattern such as surface dipole and quadrupole contribute to the force and torque on the sphere. To provide a systematic account for how a slip pattern plays a role, we extend Anderson's approach to pattern charge electrophoresis[18] to take a surface harmonic expansion for the spatially varying slip length of a non-uniform slip sphere. As will be demonstrated, this approach will allow us to develop a more general framework using the reciprocal theorem (see Sec. II) for deriving the Faxen force and torque relations in a more physics oriented form (see Secs. III and IV). The results will reveal not only how various types of forces and torques arise mainly from surface dipole and quadrupole but also that it is the antisymmetric dipole that is responsible for distinctive translation-rotation coupling. In addition, we will provide simple physical arguments in line with pictorial illustrations for explaining how these surface-moment-induced forces and torques form due to stick-slip asymmetry (see Sec. V). Impacts of the new Faxen relations by including these forces and torques will be discussed, especially when ambient flows are of non-linear type (see Sec. VI). New perspectives and outlooks will be given in the end (see Sec. VII).

II. FRAMEWORK TO ESTABLISH FORCE AND TORQUE FORMULAS USING THE RECIPROCAL THEOREM

We first construct the framework to derive the formulas for computing the hydrodynamic force and torque on a non-uniform slip sphere. This can be done below by extending the previous formulism for a uniform slip sphere[15,16] using the Lorentz reciprocal theorem.

Consider the motion of a spherical particle of radius a in an incompressible Newtonian fluid of density ρ and viscosity μ under the creeping flow condition. Let $\hat{\boldsymbol{u}}$ be the disturbance fluid velocity field and $\hat{\boldsymbol{\sigma}} = -\mathbf{I}\hat{p} + \mu(\nabla\hat{\boldsymbol{u}} + \nabla\hat{\boldsymbol{u}}^T)$ be the corresponding stress field due to the presence of the particle, where $\hat{p}$ is dynamic pressure. These fields are governed by the Stokes flow equations

$$\nabla \cdot \hat{\boldsymbol{u}} = 0, \tag{1a}$$

$$\nabla \cdot \hat{\boldsymbol{\sigma}} = 0, \tag{1b}$$

with the point-force-like characteristics $\hat{\boldsymbol{u}} \sim 1/r$ and $\hat{\boldsymbol{\sigma}} \sim 1/r^2$ when distance r to the particle becomes large compared to a. Let $(\hat{\boldsymbol{u}}_1, \hat{\boldsymbol{\sigma}}_1)$ and $(\hat{\boldsymbol{u}}_2, \hat{\boldsymbol{\sigma}}_2)$ denote the solutions for the auxiliary problem and the problem we wish to solve, respectively. They can be related by the following reciprocal relationship:[19]

$$\int_{S_p} \hat{\boldsymbol{u}}_1 \cdot (\hat{\boldsymbol{\sigma}}_2 \cdot \mathbf{n})\, \mathrm{d}S = \int_{S_p} \hat{\boldsymbol{u}}_2 \cdot (\hat{\boldsymbol{\sigma}}_1 \cdot \mathbf{n})\, \mathrm{d}S, \tag{2}$$

where S_p is the particle surface with $\mathbf{n}$ being the unit normal vector pointing into the fluid. Equation (2) will allow us to determine the force and torque for the desired problem using the solution to the auxiliary problem.

To proceed, the auxiliary problem is chosen as a uniform slip sphere having an arbitrary slip length $a\lambda$ in translational motion at velocity $\boldsymbol{U}$ and/or in rotational motion at angular velocity $\boldsymbol{\Omega}$ in a quiescent fluid [see Fig. 1(a)]. For the problem under investigation, we look at the motion of a sphere with non-uniform slip length $a\lambda'$ translating/rotating at the same velocity/angular velocity in an imposed flow $\boldsymbol{u}^\infty$ with the corresponding stress field $\boldsymbol{\sigma}^\infty$ [see Fig. 1(b)]. The perturbed flow field in this problem can be written as $(\hat{\boldsymbol{u}}_2, \hat{\boldsymbol{\sigma}}_2) = (\boldsymbol{u}_2, \boldsymbol{\sigma}_2) - (\boldsymbol{u}^\infty, \boldsymbol{\sigma}^\infty)$ in terms of the actual flow field $(\boldsymbol{u}_2, \boldsymbol{\sigma}_2)$

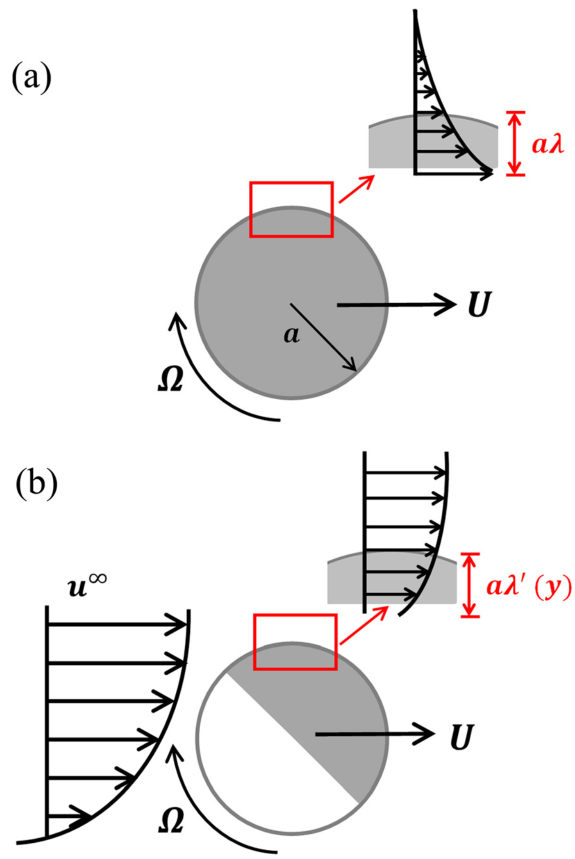

FIG. 1. Selected problems for applying the reciprocal theorem. (a) The auxiliary problem: a uniform slip sphere translating/rotating in a quiescent fluid. (b) The problem of interest: a non-uniform slip sphere moving at the same translational velocity/angular velocity in an imposed flow.

relative to the imposed flow field $(\boldsymbol{u}^\infty, \boldsymbol{\sigma}^\infty)$. For both problems, vanishing perturbed fluid velocity at infinity is imposed. Also, each is subject to the Navier-slip and the non-penetration boundary conditions on the sphere surface $|\mathbf{y}| = a$. For the known auxiliary problem, these conditions read as[16]

$$(\hat{\boldsymbol{u}}_1 - \boldsymbol{U} - \boldsymbol{\Omega}\times\mathbf{y})\cdot(\mathbf{I}-\mathbf{nn}) = \frac{a\lambda}{\mu}(\hat{\boldsymbol{\sigma}}_1\cdot\mathbf{n})\cdot(\mathbf{I}-\mathbf{nn}), \tag{3}$$

$$(\hat{\boldsymbol{u}}_1 - \boldsymbol{U} - \boldsymbol{\Omega}\times\mathbf{y})\cdot\mathbf{n} = 0. \tag{4}$$

Similarly, for the problem under investigation, the boundary conditions are

$$(\hat{\boldsymbol{u}}_2 - \boldsymbol{U} - \boldsymbol{\Omega}\times\mathbf{y} + \boldsymbol{u}^\infty)\cdot(\mathbf{I}-\mathbf{nn}) = \frac{a\lambda'(\mathbf{y})}{\mu}[(\hat{\boldsymbol{\sigma}}_2\cdot\mathbf{n}) + (\boldsymbol{\sigma}^\infty\cdot\mathbf{n})]\cdot(\mathbf{I}-\mathbf{nn}), \tag{5}$$

$$(\hat{\boldsymbol{u}}_2 - \boldsymbol{U} - \boldsymbol{\Omega}\times\mathbf{y} + \boldsymbol{u}^\infty)\cdot\mathbf{n} = \mathbf{0}. \tag{6}$$

In what follows, we will use (2)–(6) to derive the formulas for the force and torque on the sphere.

We first re-write the left-hand side of (2) as

$$\int_{S_p}\hat{\boldsymbol{u}}_1\cdot(\hat{\boldsymbol{\sigma}}_2\cdot\mathbf{n})\,dS = \int_{S_p}(\boldsymbol{U}+\boldsymbol{\Omega}\times\mathbf{y})\cdot(\hat{\boldsymbol{\sigma}}_2\cdot\mathbf{n})\,dS + \int_{S_p}(\hat{\boldsymbol{u}}_1 - \boldsymbol{U} - \boldsymbol{\Omega}\times\mathbf{y})\cdot(\hat{\boldsymbol{\sigma}}_2\cdot\mathbf{n})\,dS. \tag{7}$$

With (3) and (4), we replace $(\hat{\boldsymbol{u}}_1 - \boldsymbol{U} - \boldsymbol{\Omega}\times\mathbf{y})\cdot(\mathbf{I}-\mathbf{nn})$ in (7) by $(a\lambda/\mu)(\hat{\boldsymbol{\sigma}}_1\cdot\mathbf{n})\cdot(\mathbf{I}-\mathbf{nn})$, allowing us to re-express (7) as

$$\int_{S_p}\hat{\boldsymbol{u}}_1\cdot(\hat{\boldsymbol{\sigma}}_2\cdot\mathbf{n})\,dS = \boldsymbol{U}\cdot\int_{S_p}(\hat{\boldsymbol{\sigma}}_2\cdot\mathbf{n})\,dS + \boldsymbol{\Omega}\cdot\int_{S_p}\mathbf{y}\times(\hat{\boldsymbol{\sigma}}_2\cdot\mathbf{n})\,dS + \frac{a\lambda}{\mu}\int_{S_p}(\hat{\boldsymbol{\sigma}}_1\cdot\mathbf{n})\cdot(\mathbf{I}-\mathbf{nn})\cdot(\hat{\boldsymbol{\sigma}}_2\cdot\mathbf{n})dS. \tag{8}$$

Similarly, the right-hand side of (2) can be re-written as

$$\int_{S_p}\hat{\boldsymbol{u}}_2\cdot(\hat{\boldsymbol{\sigma}}_1\cdot\mathbf{n})\,dS = \int_{S_p}(\boldsymbol{U}+\boldsymbol{\Omega}\times\mathbf{y}-\boldsymbol{u}^\infty)\cdot(\hat{\boldsymbol{\sigma}}_1\cdot\mathbf{n})\,dS + \int_{S_p}(\hat{\boldsymbol{u}}_2 - \boldsymbol{U} - \boldsymbol{\Omega}\times\mathbf{y} + \boldsymbol{u}^\infty)\cdot(\hat{\boldsymbol{\sigma}}_1\cdot\mathbf{n})\,dS. \tag{9}$$

In the second integral, $(\hat{\boldsymbol{u}}_2 - \boldsymbol{U} - \boldsymbol{\Omega}\times\mathbf{y} + \boldsymbol{u}^\infty)\cdot(\mathbf{I}-\mathbf{nn})$ can be replaced by the slip term $(a\lambda'(\mathbf{y})/\mu)[(\hat{\boldsymbol{\sigma}}_2\cdot\mathbf{n}) + (\boldsymbol{\sigma}^\infty\cdot\mathbf{n})]\cdot(\mathbf{I}-\mathbf{nn})$ because of (5) and (6). Because λ' varies with position, we write $\lambda'(\mathbf{y}) = \lambda + (\lambda'(\mathbf{y}) - \lambda)$ and re-express (9) as

$$\begin{aligned}\int_{S_p}\hat{\boldsymbol{u}}_2\cdot(\hat{\boldsymbol{\sigma}}_1\cdot\mathbf{n})dS &= \int_{S_p}(\boldsymbol{U}+\boldsymbol{\Omega}\times\mathbf{y}-\boldsymbol{u}^\infty)\cdot(\hat{\boldsymbol{\sigma}}_1\cdot\mathbf{n})dS \\ &+ \frac{a\lambda}{\mu}\int_{S_p}\big[(\hat{\boldsymbol{\sigma}}_2\cdot\mathbf{n}) + (\boldsymbol{\sigma}^\infty\cdot\mathbf{n})\big]\cdot(\mathbf{I}-\mathbf{nn})\cdot(\hat{\boldsymbol{\sigma}}_1\cdot\mathbf{n})dS \\ &+ \frac{a}{\mu}\int_{S_p}(\lambda'(\mathbf{y})-\lambda)\big[(\hat{\boldsymbol{\sigma}}_2\cdot\mathbf{n}) + (\boldsymbol{\sigma}^\infty\cdot\mathbf{n})\big]\cdot(\mathbf{I}-\mathbf{nn})\cdot(\hat{\boldsymbol{\sigma}}_1\cdot\mathbf{n})dS.\end{aligned} \tag{10}$$

Combining (8) and (10), the two identical $(a\lambda/\mu)(\hat{\boldsymbol{\sigma}}_2\cdot\mathbf{n})\cdot(\mathbf{I}-\mathbf{nn})\cdot(\hat{\boldsymbol{\sigma}}_1\cdot\mathbf{n})$ terms are canceled out. This allows us to write the force $\boldsymbol{F} = \int_{S_p}(\hat{\boldsymbol{\sigma}}_2\cdot\mathbf{n})\,dS$ and the torque $\boldsymbol{T} = \int_{S_p}\mathbf{y}\times(\hat{\boldsymbol{\sigma}}_2\cdot\mathbf{n})\,dS$ in terms of the surface traction $(\hat{\boldsymbol{\sigma}}_1\cdot\mathbf{n})$ and the ambient flow quantities, leading (2) to

$$\begin{aligned}\boldsymbol{U}\cdot\boldsymbol{F} + \boldsymbol{\Omega}\cdot\boldsymbol{T} &= \int_{S_p}(\boldsymbol{U}+\boldsymbol{\Omega}\times\mathbf{y}-\boldsymbol{u}^\infty)\cdot(\hat{\boldsymbol{\sigma}}_1\cdot\mathbf{n})dS \\ &+ \frac{a\lambda}{\mu}\int_{S_p}(\boldsymbol{\sigma}^\infty\cdot\mathbf{n})\cdot(\mathbf{I}-\mathbf{nn})\cdot(\hat{\boldsymbol{\sigma}}_1\cdot\mathbf{n})dS \\ &+ \frac{a}{\mu}\int_{S_p}(\lambda'(\mathbf{y})-\lambda)\big[(\hat{\boldsymbol{\sigma}}_2\cdot\mathbf{n}) + (\boldsymbol{\sigma}^\infty\cdot\mathbf{n})\big] \\ &\cdot(\mathbf{I}-\mathbf{nn})\cdot(\hat{\boldsymbol{\sigma}}_1\cdot\mathbf{n})dS.\end{aligned} \tag{11}$$

In (11), the last term accounts for the contribution from spatial variations $a(\lambda'(\mathbf{y}) - \lambda)$ in the slip length. As will be shown shortly, it is this term responsible for coupling between translation and rotation. Since it involves the unknown traction $(\hat{\boldsymbol{\sigma}}_2\cdot\mathbf{n})$, we determine both $\boldsymbol{F}$ and $\boldsymbol{T}$ approximately by assuming that $a|\lambda'(\mathbf{y}) - \lambda|$ is small compared to the average slip length $a\langle\lambda'\rangle$. Define $\varepsilon f(\mathbf{y}) \equiv \lambda'(\mathbf{y}) - \langle\lambda'\rangle$ where $\varepsilon \ll 1$ measures the amplitude of slip anisotropy described by an $O(1)$ function $f(\mathbf{y})$. Also, for simplicity, $\langle\lambda'\rangle$ is assumed $O(1)$. We further assign λ, the dimensionless slip length for the auxiliary uniform-slip problem, to be equal to $\langle\lambda'\rangle$. Thus, we can express $\lambda'(\mathbf{y})$ as

$$\lambda'(\mathbf{y}) = \langle\lambda'\rangle + \varepsilon f(\mathbf{y}) = \lambda + \varepsilon f(\mathbf{y}). \tag{12}$$

Equation (12) can also be applied to the weakly stick–slip situation where $\langle\lambda'\rangle = O(\varepsilon)$. In this case, we can take the fluid motion around a no-slip sphere as the auxiliary problem to which slip is a small perturbation.

With $\varepsilon \ll 1$ in (12), the unknown traction $(\hat{\boldsymbol{\sigma}}_2\cdot\mathbf{n})$ in (11) can be expanded as $(\hat{\boldsymbol{\sigma}}_2\cdot\mathbf{n}) = (\hat{\boldsymbol{\sigma}}_2^{(0)}\cdot\mathbf{n}) + (\hat{\boldsymbol{\sigma}}_2^{(1)}\cdot\mathbf{n}) + \cdots$ with a correction $(\hat{\boldsymbol{\sigma}}_2^{(1)}\cdot\mathbf{n})$ of $O(\varepsilon)$ to the uniform-slip problem. In other words, we seek the impacts of slip non-uniformity on (11) up to $O(\varepsilon)$ by keeping the slip variation integral accurate to $O(\varepsilon)$ with

$$(\hat{\boldsymbol{\sigma}}_2\cdot\mathbf{n}) = (\hat{\boldsymbol{\sigma}}_2^{(0)}\cdot\mathbf{n}) + O(\varepsilon). \tag{13}$$

Similar perturbation approaches have been employed to solve a variety of problems.[20–23] Using the stress field of an unperturbed problem to approximate the unknown stress field of a desired problem due to small perturbation in the reciprocal theorem formulation has been shown to provide a simpler way to compute the hydrodynamic force and torque for the latter without having to solve detailed flow fields.[22]

To derive the formulas for $\boldsymbol{F}$ and $\boldsymbol{T}$ from (11), it is more convenient to write $(\hat{\boldsymbol{\sigma}}_2^{(0)}\cdot\mathbf{n})$ in terms of translation resistance tensor $\boldsymbol{R}^T$ and rotation resistance tensor $\boldsymbol{R}^R$,

$$(\hat{\boldsymbol{\sigma}}_2^{(0)}\cdot\mathbf{n}) = \mu\boldsymbol{R}^T\cdot(\boldsymbol{U} - \boldsymbol{u}^\infty(\mathbf{x_p})) + \mu\boldsymbol{R}^R\cdot\big((\boldsymbol{\Omega} - \boldsymbol{\Omega}^\infty(\mathbf{x_p}))\times\mathbf{y}\big). \tag{14}$$

The two resistance tenors $\boldsymbol{R}^T$ and $\boldsymbol{R}^R$ here are constructed in proportional to the sphere's velocity $(\boldsymbol{U} - \boldsymbol{u}^\infty(\mathbf{x_p}))$ and angular velocity $(\boldsymbol{\Omega} - \boldsymbol{\Omega}^\infty(\mathbf{x_p}))$ relative to the imposed flow. $\boldsymbol{u}^\infty$ is the imposed flow field, $\boldsymbol{\Omega}^\infty = (1/2)(\nabla\times\boldsymbol{u}^\infty)$ is half the vorticity of the imposed flow, and both are evaluated at the sphere's center at $\mathbf{x_p}$. For a uniform slip sphere, these resistance tensors are given by[16]

$$\boldsymbol{R}^T = \frac{-1}{a}\left[\frac{3/2}{1+3\lambda}\right]\mathbf{I} - \frac{1}{a}\left[\frac{9\lambda}{1+3\lambda}\right]\mathbf{nn}, \tag{15a}$$

$$\boldsymbol{R}^R = \frac{-1}{a}\left[\frac{3}{1+3\lambda}\right]\mathbf{I}. \tag{15b}$$

Substituting (13) and (14) into (11), we keep the terms up to $O(\varepsilon)$. Furthermore, by making use of the linearity of the Stokes flow, we convert (11) into a matrix representation to re-express $\boldsymbol{F}$ and $\boldsymbol{T}$ in a bilinear form of $\boldsymbol{U}$ and $\boldsymbol{\Omega}$,

$$[\,\boldsymbol{U}\,,\,\boldsymbol{\Omega}\,]\begin{bmatrix}\boldsymbol{F}-\boldsymbol{F}^\infty\\ \boldsymbol{T}-\boldsymbol{T}^\infty\end{bmatrix} = \mu[\,\boldsymbol{U}\,,\,\boldsymbol{\Omega}\,]\begin{bmatrix}\boldsymbol{R}_{FU} & \boldsymbol{R}_{F\boldsymbol{\Omega}}\\ \boldsymbol{R}_{TU} & \boldsymbol{R}_{T\boldsymbol{\Omega}}\end{bmatrix}\begin{bmatrix}\boldsymbol{U}-\boldsymbol{u}^\infty(\mathbf{x_p})\\ \boldsymbol{\Omega}-\boldsymbol{\Omega}^\infty(\mathbf{x_p})\end{bmatrix}, \tag{16}$$

$$\begin{aligned}
\boldsymbol{F}^\infty &= a\lambda\int_{S_p}\boldsymbol{R}_{\|}^T\cdot(\boldsymbol{\sigma}^\infty\cdot\mathbf{n})\,\mathrm{d}S - \mu\int_{S_p}\boldsymbol{u}^\infty\cdot\boldsymbol{R}^T\,\mathrm{d}S\\
&\quad+\varepsilon a\int_{S_p} f(\mathbf{y})\boldsymbol{R}_{\|}^T\cdot(\boldsymbol{\sigma}^\infty\cdot\mathbf{n})\,\mathrm{d}S,\\
\boldsymbol{T}^\infty &= a\lambda\int_{S_p}\mathbf{y}\times\left[\boldsymbol{R}_{\|}^R\cdot(\boldsymbol{\sigma}^\infty\cdot\mathbf{n})\right]\mathrm{d}S - \mu\int_{S_p}\mathbf{y}\times(\boldsymbol{R}^R\cdot\boldsymbol{u}^\infty)\,\mathrm{d}S\\
&\quad+\varepsilon a\int_{S_p} f(\mathbf{y})\mathbf{y}\times\left[\boldsymbol{R}_{\|}^R\cdot(\boldsymbol{\sigma}^\infty\cdot\mathbf{n})\right]\mathrm{d}S,\\
\boldsymbol{R}_{FU} &= \mu\int_{S_p}\boldsymbol{R}^T\,\mathrm{d}S + \varepsilon a\mu\int_{S_p} f(\mathbf{y})\boldsymbol{R}^T\cdot\boldsymbol{R}_{\|}^T\,\mathrm{d}S,\\
\boldsymbol{R}_{F\boldsymbol{\Omega}} &= \varepsilon a\mu\int_{S_p} f(\mathbf{y})\boldsymbol{R}^T\cdot(\mathbf{y}\times\boldsymbol{R}_{\|}^R)\,\mathrm{d}S,\\
\boldsymbol{R}_{TU} &= \varepsilon a\mu\int_{S_p} f(\mathbf{y})\mathbf{y}\times(\boldsymbol{R}^R\cdot\boldsymbol{R}_{\|}^T)\,\mathrm{d}S,\\
\boldsymbol{R}_{T\boldsymbol{\Omega}} &= \mu\int_{S_p}\mathbf{y}\times(\mathbf{y}\times\boldsymbol{R}^R)\,\mathrm{d}S + \varepsilon a\mu\int_{S_p} f(\mathbf{y})\mathbf{y}\times\left[\boldsymbol{R}^R\cdot(\mathbf{y}\times\boldsymbol{R}_{\|}^R)\right]\mathrm{d}S.
\end{aligned} \tag{17}$$

In the above, $\boldsymbol{R}_{\|}\equiv(\mathbf{I}-\mathbf{nn})\cdot\boldsymbol{R}$ is the tangential projection of resistance tensor. $\boldsymbol{R}_{FU}$ is found symmetric, and so is $\boldsymbol{R}_{T\boldsymbol{\Omega}}$ [in view of (15b)]. The coupling tensors $\boldsymbol{R}_{F\boldsymbol{\Omega}}$ and $\boldsymbol{R}_{TU}$ also satisfy $\boldsymbol{R}_{F\boldsymbol{\Omega}} = (\boldsymbol{R}_{TU})^T$. In fact, the symmetries between these tensors are consequences of the reciprocal theorem.[22–25] Because $[\boldsymbol{F},\boldsymbol{T}]^T$ has to be linear in $[\boldsymbol{U}-\boldsymbol{u}^\infty(\mathbf{x_p}),\boldsymbol{\Omega}-\boldsymbol{\Omega}^\infty(\mathbf{x_p})]^T$ and also because $\boldsymbol{U}$ and $\boldsymbol{\Omega}$ are independent and their choices are arbitrary, (16) without $[\boldsymbol{U},\boldsymbol{\Omega}]$ in the front of both sides must always hold. Similar to Oppenheimer *et al.*,[22] we can eliminate the front $[\boldsymbol{U},\boldsymbol{\Omega}]$ in (16) to obtain

$$\begin{bmatrix}\boldsymbol{F}-\boldsymbol{F}^\infty\\ \boldsymbol{T}-\boldsymbol{T}^\infty\end{bmatrix} = \mu\begin{bmatrix}\boldsymbol{R}_{FU} & \boldsymbol{R}_{F\boldsymbol{\Omega}}\\ \boldsymbol{R}_{TU} & \boldsymbol{R}_{T\boldsymbol{\Omega}}\end{bmatrix}\begin{bmatrix}\boldsymbol{U}-\boldsymbol{u}^\infty(\mathbf{x_p})\\ \boldsymbol{\Omega}-\boldsymbol{\Omega}^\infty(\mathbf{x_p})\end{bmatrix}. \tag{18}$$

For clarity, we split $(\boldsymbol{F},\boldsymbol{T})$ above into the uniform-slip part $(\boldsymbol{F}_0,\boldsymbol{T}_0)$ and the $O(\varepsilon)$ non-uniform slip part $(\boldsymbol{F}',\boldsymbol{T}')$ as follows:

$$\boldsymbol{F} = \boldsymbol{F}_0 + \boldsymbol{F}', \tag{19a}$$

$$\boldsymbol{F_0} = \mu\int_{S_p}(\boldsymbol{U}-\boldsymbol{u}^\infty)\cdot\boldsymbol{R}^T\,\mathrm{d}S + a\lambda\int_{S_p}\boldsymbol{R}_{\|}^T\cdot(\boldsymbol{\sigma}^\infty\cdot\mathbf{n})\mathrm{d}S, \tag{19b}$$

$$\begin{aligned}
\boldsymbol{F}' = \varepsilon a\mu\Bigg[&\int_{S_p} f(\mathbf{y})\,\boldsymbol{R}^T\cdot\left[\boldsymbol{R}_{\|}^T\cdot(\boldsymbol{U}-\boldsymbol{u}^\infty(\mathbf{x_p}))\right]\mathrm{d}S\\
&+\int_{S_p} f(\mathbf{y})\,\boldsymbol{R}^T\cdot\left[\boldsymbol{R}_{\|}^R\cdot((\boldsymbol{\Omega}-\boldsymbol{\Omega}^\infty(\mathbf{x_p}))\times\mathbf{y})\right]\mathrm{d}S\\
&+\int_{S_p}\mu^{-1}f(\mathbf{y})\,\boldsymbol{R}_{\|}^T\cdot(\boldsymbol{\sigma}^\infty\cdot\mathbf{n})\,\mathrm{d}S\Bigg].
\end{aligned} \tag{19c}$$

$$\boldsymbol{T} = \boldsymbol{T}_0 + \boldsymbol{T}', \tag{20a}$$

$$\begin{aligned}
\boldsymbol{T}_0 &= \int_{S_p}\mathbf{y}\times\left[\boldsymbol{R}^R\cdot(\boldsymbol{\Omega}\times\mathbf{y}-\boldsymbol{u}^\infty)\right]\mathrm{d}S\\
&\quad+a\lambda\int_{S_p}\mathbf{y}\times\left[\boldsymbol{R}_{\|}^R\cdot(\boldsymbol{\sigma}^\infty\cdot\mathbf{n})\right]\mathrm{d}S,
\end{aligned} \tag{20b}$$

$$\begin{aligned}
\boldsymbol{T}' = \varepsilon a\mu\Bigg[&\int_{S_p} f(\mathbf{y})\,\mathbf{y}\times\left[\boldsymbol{R}^R\cdot(\boldsymbol{R}_{\|}^R\cdot((\boldsymbol{\Omega}-\boldsymbol{\Omega}^\infty(\mathbf{x_p}))\times\mathbf{y}))\right]\mathrm{d}S\\
&+\int_{S_p} f(\mathbf{y})\,\mathbf{y}\times\left[\boldsymbol{R}^R\cdot(\boldsymbol{R}_{\|}^T\cdot(\boldsymbol{U}-\boldsymbol{u}^\infty(\mathbf{x_p})))\right]\mathrm{d}S\\
&+\int_{S_p}\mu^{-1}f(\mathbf{y})\,\mathbf{y}\times\left[\boldsymbol{R}_{\|}^R\cdot(\boldsymbol{\sigma}^\infty\cdot\mathbf{n})\right]\mathrm{d}S\Bigg].
\end{aligned} \tag{20c}$$

Equations (19) and (20) provide the formulas for computing the hydrodynamic force $\boldsymbol{F}$ and torque $\boldsymbol{T}$ exerted on a non-uniform slip sphere. Inclusion of both leading order and $O(\varepsilon)$ contributions in the formulation here is similar to what Swan and Khair[17] did in their integral representation of the Faxen relations. However, to better see how these ε terms in (19) and (20) contribute to the additional force $\boldsymbol{F}'$ and torque $\boldsymbol{T}'$ for a given non-uniform slip length $\lambda'(\mathbf{y})$, it is necessary to expand $\lambda'(\mathbf{y})$ in terms of surface spherical harmonics. This essentially decomposes $\lambda'(\mathbf{y})$ into a combination of surface moments, such as dipole, quadrupole, and octupole. Since these surface moments represent either even or odd distributions with distinct polarities over a sphere, this approach will offer a more systematic way to reveal how slip anisotropy breaks spherical symmetry in affecting the force and torque on the sphere. More importantly, these surface moments can be readily incorporated into tensor calculus for computing the force and torque.

III. SURFACE HARMONIC EXPANSION FOR A NON-UNIFORM SLIP DISTRIBUTION

Following the preceding section, prior to deriving the Faxen relations, we follow Anderson[18] to expand the spatially varying slip length $\lambda'(\mathbf{y})$ as a series of surface spherical harmonics,

$$\lambda'(\mathbf{y}) = \sum_m (a/r)^{m+1}A_m[\cdot]\mathbf{S}_m. \tag{21}$$

Here, the m-th order polyadic $\mathbf{S}_m$ is the set of surface spherical harmonics,

$$\mathbf{S}_m \equiv r^{m+1}(\nabla\cdots\nabla)^m(r^{-1}),$$

giving $S_0 = 1$, $\mathbf{S}_1 = -\mathbf{n}$, $\mathbf{S}_2 = 3\mathbf{nn}-\mathbf{I}$, etc. A_m are the coefficients to form a scalar product with $\mathbf{S}_m$ through operator $[\cdot]$. These coefficients can be determined by applying the orthogonal relationships between these surface harmonics according to

$$\langle\mathbf{S}_m\mathbf{S}_k\rangle = 1/(4\pi a^2)\int_{Sp}\mathbf{S}_m\mathbf{S}_k\mathrm{d}S, \tag{22}$$

which is non-zero if $m=k$ and zero otherwise. Here, $\langle\cdots\rangle = 1/(4\pi a^2)\int_{S_p}(\cdots)\mathrm{d}S$ is the average over the sphere's surface. The first few of these orthogonal relationships are

$$\langle S_0 S_0 \rangle = 1,$$
$$\langle \mathbf{S}_1 \mathbf{S}_1 \rangle_{ij} = \frac{1}{3}\delta_{ij},$$
$$\langle \mathbf{S}_2 \mathbf{S}_2 \rangle_{ijkl} = \frac{1}{5}\left(-2\delta_{ij}\delta_{kl} + 3\delta_{ik}\delta_{jl} + 3\delta_{il}\delta_{jk}\right).$$

Using (22), we can express (21) in terms of monopole (surface average) $\langle \lambda' S_0 \rangle = \langle \lambda' \rangle (= \lambda)$, surface dipole $\mathbf{P}_1 \equiv -\langle \lambda' \mathbf{S}_1 \rangle$, surface quadrupole $\mathbf{P}_2 \equiv \langle \lambda' \mathbf{S}_2 \rangle$, etc.: $\lambda'(\mathbf{y}) = \langle \lambda' \rangle - 3\mathbf{P}_1 \cdot \mathbf{S}_1 + (5/6)\mathbf{P}_2 : \mathbf{S}_2 + \cdots$, or

$$\varepsilon f(\mathbf{y}) = -3\mathbf{P}_1 \cdot \mathbf{S}_1 + (5/6)\mathbf{P}_2 : \mathbf{S}_2 + \cdots \tag{23}$$

after subtracting $\langle \lambda' \rangle$. Note that $\langle \mathbf{S}_m \rangle = 0$ except for the average mode $m = 0$ because of the orthogonality between $m \neq 0$ and $k = 0$ according to (22). Here, we assume that the slip length varies spatially in a scale of sphere's size or larger. This will ensure that effects of slip anisotropy can be fairly captured by the first few surface harmonic contributions without having to include high harmonic contributions. Also, given that a spherical Janus particle is typically of two-faced or of striped type,[18] it suffices to consider the first two-surface harmonics: dipole $\mathbf{P}_1$ and quadrupole $\mathbf{P}_2$. Dipole $\mathbf{P}_1$ can be pictured as a half-faced pattern, representing the first odd surface harmonic mode. Quadrupole $\mathbf{P}_2$ represents the first (non-zero) even surface harmonic mode, describing a dipolar pattern with two equal caps at the poles. Thus, if a slip–slip Janus sphere is made of two unequal faces, it can be thought of as a uniform-slip sphere with $\langle \lambda' \rangle$ plus a linear superposition of first odd $\mathbf{P}_1$ and even $\mathbf{P}_2$ modes due to slip anisotropy, as illustrated in Fig. 2(a).

As either two-faced type or striped type possesses a polarity represented by a stick-slip director $\mathbf{d}$, it is more convenient to form $\mathbf{P}_1$ and $\mathbf{P}_2$ in terms of $\mathbf{d}$. To this end, we can re-construct (23) in terms of $\mathbf{d}$ and $\mathbf{dd}$ as

$$\varepsilon f(\mathbf{y}) = 3\mathscr{D}\mathbf{d} \cdot \mathbf{S}_1 + (5/2)\mathscr{Q}\mathbf{dd} : \mathbf{S}_2 + \cdots. \tag{24}$$

Thus, the surface moments $\mathbf{P}_1$ and $\mathbf{P}_2$ in (23) can be expressed in terms of $\mathbf{d}$ with the coefficients $\mathscr{D}$ and $\mathscr{Q}$ measuring the strengths of these surface moments,

$$\mathbf{P}_1 \equiv -\varepsilon \langle f \mathbf{S}_1 \rangle = \mathscr{D}\,\mathbf{d}, \tag{25a}$$
$$\mathbf{P}_2 \equiv \varepsilon \langle f \mathbf{S}_2 \rangle = \mathscr{Q}(3\mathbf{dd} - \mathbf{I}). \tag{25b}$$

Note that both $\mathscr{D}$ and $\mathscr{Q}$ are $O(\varepsilon)$ because of $\varepsilon f(\mathbf{y})$ in (24).

To illustrate how $\mathbf{P}_1$ and $\mathbf{P}_2$ are determined by a given slip length distribution, we assume that the distribution is axisymmetric so that it can be expressed as a Legendre series,

$$\lambda' = g_0 P_0 + g_1 P_1(\eta) + g_2 P_2(\eta) + \cdots. \tag{26}$$

Here, $P_0(\eta) = 1, P_1(\eta) = \eta, P_2(\eta) = (3\eta^2 - 1)/2$, etc., are the Legendre polynomials with $\eta = \cos\theta$ in terms of the polar angle θ with respect to the symmetry axis, and the coefficients g_n are given by $g_\mathbf{n} = (\mathbf{n} + 1/2)\int_{-1}^{1} \lambda' P_\mathbf{n}(\eta) d\eta$. In connection to (23) we have $\langle \lambda' \rangle = g_0, \mathscr{D} = g_1/3$ and $\mathscr{Q} = g_2/5$. For a two-faced Janus sphere with slip lengths λ^+ and λ^-, it has

$$\begin{aligned} \langle \lambda' \rangle &= (1/2)\left((\lambda^- - \lambda^+)\cos\alpha + \lambda^+ + \lambda^-\right), \\ \mathscr{D} &= (1/4)(\lambda^+ - \lambda^-)\sin^2\alpha, \\ \mathscr{Q} &= (1/4)(\lambda^+ - \lambda^-)\sin^2\alpha\cos\alpha, \end{aligned} \tag{27}$$

where α is the dividing angle for the more slippery λ^+ part. Note that both $\mathscr{D}$ and $\mathscr{Q}$ are proportional to $(\lambda^+ - \lambda^-)$ of $O(\varepsilon)$. Also, $\mathscr{Q} = \mathscr{D}\cos\alpha$ indicates that surface dipole $\mathbf{P}_1$ is generally more dominant than surface quadrupole $\mathbf{P}_2$. For a symmetric slip–stick–slip sphere having two more slippery caps in equal size (of dividing angles α and $\pi - \alpha$) and a less slippery stripe in the middle, we have

$$\begin{aligned} \langle \lambda' \rangle &= \lambda^+(1 - \cos\alpha) + \lambda^- \cos\alpha, \\ \mathscr{D} &= 0, \\ \mathscr{Q} &= (1/2)(\lambda^+ - \lambda^-)\sin^2\alpha\cos\alpha. \end{aligned} \tag{28}$$

Thus, the non-uniform slip part of this case is completely governed by $\mathbf{P}_2$ with $\mathscr{Q} > 0$ pointing outward. Because of the less hydrodynamic resistance on the two more slippery poles, such a slip–stick–slip sphere may act like a prolate spheroid. Similarly, for a symmetric stick–slip–stick sphere, it is characterized by $\mathbf{P}_2$ with $\mathscr{Q} < 0$ pointing inward in

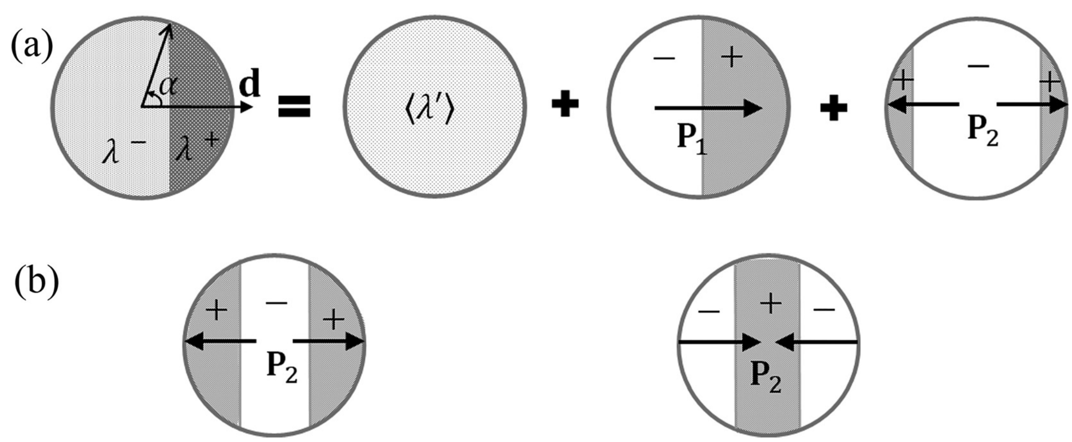

FIG. 2. (a) The slip length distribution of a slip-slip Janus sphere can be represented by its average slip length plus a linear combination of odd and even contributions represented, respectively, by surface dipole $\mathbf{P}_1$ and quadrupole $\mathbf{P}_2$. (b) Symmetric slip–stick–slip and stick–slip–stick spheres can be represented by outward and inward quadrupoles, respectively.

analogy to an oblate spheroid. Figure 2(b) illustrates these dipolar Janus spheres represented by outward and inward surface quadrupoles.

It is worth re-stating that we are mainly looking at the first order effects of slip anisotropy at $O(\varepsilon)$. Possible non-linear interactions or coupling between different surface harmonics may occur at higher orders and, hence, can be negligible here.

IV. COUPLED FAXEN FORCE AND TORQUE RELATIONS FOR A NON-UNIFROM SLIP JANUS SPHERE

Now, we are in the position to evaluate force (19) and torque (20). We first expand $\boldsymbol{u}^\infty$ and $\boldsymbol{\sigma}^\infty$ with respect to the sphere's center located at $\mathbf{x} = \mathbf{x_p}$ as

$$\boldsymbol{u}^\infty = \boldsymbol{u}^\infty(\mathbf{x}_p) + \mathbf{y}\cdot\nabla\boldsymbol{u}^\infty|_{\mathbf{x}_p} + \frac{\mathbf{y}\,\mathbf{y}}{2!} : \nabla\nabla\boldsymbol{u}^\infty|_{\mathbf{x}_p} + \cdots, \tag{29a}$$

$$\boldsymbol{\sigma}^\infty = \boldsymbol{\sigma}^\infty(\mathbf{x}_p) + \mathbf{y}\cdot\nabla\boldsymbol{\sigma}^\infty|_{\mathbf{x}_p} + \frac{\mathbf{y}\,\mathbf{y}}{2!} : \nabla\nabla\boldsymbol{\sigma}^\infty|_{\mathbf{x}_p} + \frac{\mathbf{y}\,\mathbf{y}\,\mathbf{y}}{3!} \vdots \nabla\nabla\nabla\boldsymbol{\sigma}^\infty|_{\mathbf{x}_p} + \cdots, \tag{29b}$$

where $\mathbf{y} = \mathbf{x} - \mathbf{x}_p$.

Substituting (23), (15), and (29) into (19) and (20), the evaluations of various integrals in (19) and (20) require the following identities involving even surface moments:

$$\int_{S_p} \mathbf{n}_i\mathbf{n}_j \mathrm{d}S = (4/3)\pi a^2 \delta_{ij}, \tag{30a}$$

$$\int_{S_p} \mathbf{n}_i\mathbf{n}_j\mathbf{n}_k\mathbf{n}_m \mathrm{d}S = (4/15)\pi a^2 A_{ijkm}, \tag{30b}$$

$$\int_{S_p} \mathbf{n}_p\mathbf{n}_q\mathbf{n}_i\mathbf{n}_j\mathbf{n}_k\mathbf{n}_m \mathrm{d}S = (4/105)\pi a^2 B_{pqijkm}, \tag{30c}$$

$$\int_{S_p} \mathbf{n}_p\mathbf{n}_q\mathbf{n}_i\mathbf{n}_j\mathbf{n}_k\mathbf{n}_m\mathbf{n}_n\mathbf{n}_l \mathrm{d}S = (4/945)\pi a^2 C_{pqijkmnl}, \tag{30d}$$

where $A_{ijkm} = \delta_{ij}\delta_{km} + \delta_{ik}\delta_{jm} + \delta_{im}\delta_{jk}$, $B_{pqijkm} = \delta_{pq}A_{ijkm} + \delta_{pi}A_{qjkm} + \delta_{pj}A_{iqkm} + \delta_{pk}A_{ijqm} + \delta_{pm}A_{ijkq}$, and $C_{pqijkmnl} = \delta_{km}B_{pqijnl} + \delta_{kn}B_{pqijml} + \delta_{kl}B_{pqijnm} + \delta_{kp}B_{mqijnl} + \delta_{kq}B_{pmijnl} + \delta_{ki}B_{pqmjnl} + \delta_{kj}B_{pqimnl}$.

In the following, we merely present main results and provide detailed derivations in Appendixes A and B.

A. Faxen force relation

The force given by (19) is made of the uniform slip part $\boldsymbol{F}_0$ and non-uniform slip part $\boldsymbol{F}'$. The former is the usual Faxen force relation,

$$\boldsymbol{F}_0 = -6\pi\mu a\Lambda\left[\boldsymbol{U} - \left(1 + \frac{a^2}{6(1+2\lambda)}\nabla^2\right)\right]\boldsymbol{u}^\infty(\mathbf{x}_p), \tag{31}$$

with $\Lambda = (1+2\lambda)/(1+3\lambda)$ being the Hadamard–Rybczynski factor in analogy to the Stokes drag on a spherical drop.[12,16] Equation (31) recovers the Faxen force law for uniform-slip spheres.[15,16] Its derivation is standard, which involves the use of (30a) and (30b) [see (A2b), (A3), and (A4)].

The $O(\varepsilon)$ non-uniform slip part $\boldsymbol{F}' = \boldsymbol{F}'_D + \boldsymbol{F}'_Q$ consists of the dipole force $\boldsymbol{F}'_D$ and the quadrupole force $\boldsymbol{F}'_Q$. Each force involves contributions from both the imposed flow and the body movements. These forces are found to be

$$\begin{aligned}\boldsymbol{F}'_D \equiv\; &\varepsilon a\int_{S_p} 3[\langle f\mathbf{S}_1\rangle\cdot\mathbf{S}_1]\boldsymbol{R}_{||}^T\cdot\left(\boldsymbol{\sigma}^\infty|_{\mathbf{x}_p} + \frac{\mathbf{y}\mathbf{y}}{2!}:\nabla\nabla\boldsymbol{\sigma}^\infty|_{\mathbf{x}_p} + \cdots\right)\cdot\mathbf{n}\,\mathrm{d}S\\ &+\varepsilon a\mu\int_{S_p} 3[\langle f\mathbf{S}_1\rangle\cdot\mathbf{S}_1]\boldsymbol{R}^T\cdot(\boldsymbol{R}_{||}^R\cdot((\boldsymbol{\Omega}-\boldsymbol{\Omega}^\infty(\mathbf{x}_p))\times\mathbf{y}))\mathrm{d}S\\ =\;&\frac{18\pi\mu a^2}{(1+3\lambda)^2}(\boldsymbol{\Omega}-\boldsymbol{\Omega}^\infty(\mathbf{x}_p))\times\mathbf{P}_1\\ &-\frac{36}{5}\frac{\pi\mu a^2}{(1+3\lambda)}\left(1+\frac{5a^2}{42}\nabla^2\right)\boldsymbol{E}^\infty(\mathbf{x}_p)\cdot\mathbf{P}_1\\ &+\frac{6}{35}\frac{\pi a^4}{(1+3\lambda)}\nabla\nabla\sigma_{jj}^\infty|_{\mathbf{x}_p}\cdot\mathbf{P}_1,\end{aligned} \tag{32}$$

$$\begin{aligned}\boldsymbol{F}'_Q \equiv\; &\varepsilon a\int_{S_p}(5/6)[\langle f\mathbf{S}_2\rangle : \mathbf{S}_2]\,\boldsymbol{R}_{||}^T\\ &\cdot\left(\mathbf{y}\cdot\nabla\boldsymbol{\sigma}^\infty|_{\mathbf{x}_p} + \frac{\mathbf{y}\mathbf{y}\mathbf{y}}{3!}\vdots\nabla\nabla\nabla\boldsymbol{\sigma}^\infty|_{\mathbf{x}_p} + \cdots\right)\cdot\mathbf{n}\,\mathrm{d}S\\ &+\varepsilon a\mu\int_{S_p}(5/6)[\langle f\mathbf{S}_2\rangle : \mathbf{S}_2]\,\boldsymbol{R}^T\cdot\boldsymbol{R}_{||}^T\cdot(\boldsymbol{U}-\boldsymbol{u}^\infty(\mathbf{x}_p))\mathrm{d}S\\ =\;&-\frac{3\pi\mu a}{(1+3\lambda)^2}\mathbf{P}_2\cdot(\boldsymbol{U}-\boldsymbol{u}^\infty(\mathbf{x}_p)) - \frac{10}{7}\frac{\pi a^3}{(1+3\lambda)}\left(1+\frac{7a^2}{90}\nabla^2\right)\\ &\nabla\boldsymbol{\sigma}^\infty|_{\mathbf{x}_p} : \mathbf{P}_2 + \frac{2}{7}\frac{\pi a^3}{(1+3\lambda)}\left(1+\frac{a^2}{18}\nabla^2\right)\nabla\left(\boldsymbol{\sigma}^\infty|_{\mathbf{x}_p} : \mathbf{P}_2\right)\\ &+\frac{2}{7}\frac{\pi a^3}{(1+3\lambda)}\nabla\sigma_{jj}^\infty|_{\mathbf{x}_p}\cdot\mathbf{P}_2.\end{aligned} \tag{33}$$

Here, $\boldsymbol{E}^\infty = (1/2)(\nabla\boldsymbol{u}^\infty + \nabla\boldsymbol{u}^{\infty\,T})$ is the local rate of strain tensors. For deriving (32), we have used (30a)–(30c) for computing the integrals. Equation (33) can be obtained after simplifying the integral with (30a)–(30d). More details are given in (A5)–(A13).

Combining (31)–(33), we arrive at the Faxen force relation,

$$\begin{aligned}\boldsymbol{F} =\; &-6\pi\mu a\Lambda\left[\boldsymbol{U} - \left(1+\frac{a^2}{6(1+2\lambda)}\nabla^2\right)\boldsymbol{u}^\infty(\mathbf{x}_p)\right.\\ &\left.+\frac{1/2}{(1+2\lambda)(1+3\lambda)}\mathbf{P}_2\cdot(\boldsymbol{U}-\boldsymbol{u}^\infty(\mathbf{x}_p))\right]\\ &+\frac{18\pi\mu a^2}{(1+3\lambda)^2}(\boldsymbol{\Omega}-\boldsymbol{\Omega}^\infty(\mathbf{x}_p))\times\mathbf{P}_1 - \frac{36}{5}\frac{\pi\mu a^2}{(1+3\lambda)}\\ &\times\left(1+\frac{5a^2}{42}\nabla^2\right)\boldsymbol{E}^\infty(\mathbf{x}_p)\cdot\mathbf{P}_1 + \frac{6}{35}\frac{\pi a^4}{1+3\lambda}\nabla\nabla\sigma_{jj}^\infty|_{\mathbf{x}_p}\cdot\mathbf{P}_1\\ &-\frac{10}{7}\frac{\pi a^3}{(1+3\lambda)}\left(1+\frac{7a^2}{90}\nabla^2\right)\nabla\boldsymbol{\sigma}^\infty|_{\mathbf{x}_p} : \mathbf{P}_2\\ &+\frac{2}{7}\frac{\pi a^3}{(1+3\lambda)}\left(1+\frac{a^2}{18}\nabla^2\right)\nabla(\boldsymbol{\sigma}^\infty|_{\mathbf{x}_p} : \mathbf{P}_2)\\ &+\frac{2}{7}\frac{\pi a^3}{(1+3\lambda)}\nabla\sigma_{jj}^\infty|_{\mathbf{x}_p}\cdot\mathbf{P}_2.\end{aligned} \tag{34}$$

As indicated by (34), non-uniform slip can bring four additional forces through surface moments $\mathbf{P}_1$ and $\mathbf{P}_2$ at $O(\varepsilon)$: (i) the quadrupole drag through $\mathbf{P}_2$, (ii) the dipole force from the linear (straining) part of the imposed flow through $\mathbf{P}_1$, (iii) the quadrupole force from the quadratic part of the imposed flow through $\mathbf{P}_2$, and (iv) the force due to rotational coupling through $\mathbf{P}_1$. In (ii) and (iii), higher order Faxen corrections can exist when the imposed flow gradient becomes non-uniform. This can be the case for the multi-particle situation where a non-uniform slip sphere is surrounded by other particles in motion, and the former can be subjected to a flow caused by the latter.

Since (34) contains both the non-uniform slip contributions of $O(\varepsilon)$ and the finite-size correction terms of $O((a/L)^2)$ or smaller (with L being the macroscopic length over which flow gradients occur), the latter can be negligible compared to the former if

$$\varepsilon \gg (a/L)^2. \tag{35}$$

Under the above condition, we can neglect the finite-size correction terms $\nabla^2 \boldsymbol{E}^\infty(\mathbf{x_p})\cdot\mathbf{P}_1$, $\nabla\nabla\boldsymbol{\sigma}^\infty_{jj}|_{\mathbf{x_p}}\cdot\mathbf{P}_1$, $\nabla\boldsymbol{\sigma}^\infty|_{\mathbf{x_p}}:\mathbf{P}_2$, $\nabla(\boldsymbol{\sigma}^\infty|_{\mathbf{x_p}}:\mathbf{P}_2)$ and $\nabla\boldsymbol{\sigma}^\infty_{jj}|_{\mathbf{x_p}}\cdot\mathbf{P}_2$ in (34) due to non-uniform flow gradients, which simplifies (34) to

$$\boldsymbol{F} = -6\pi\mu a\Lambda\left(\mathbf{I}+\frac{1/2}{(1+2\lambda)(1+3\lambda)}\mathbf{P}_2\right)\cdot(\boldsymbol{U}-\boldsymbol{u}^\infty(\mathbf{x_p})) + \frac{18\pi\mu a^2}{(1+3\lambda)^2}(\boldsymbol{\Omega}-\boldsymbol{\Omega}^\infty(\mathbf{x_p}))\times\mathbf{P}_1 - \frac{36}{5}\frac{\pi\mu a^2}{(1+3\lambda)}\boldsymbol{E}^\infty(\mathbf{x_p})\cdot\mathbf{P}_1. \tag{36}$$

As a result, quadrupole $\mathbf{P}_2$ will contribute a correction $\mathbf{P}_2\cdot(\boldsymbol{U}-\boldsymbol{u}^\infty(\mathbf{x_p}))$ to the Stokes drag. Dipole $\mathbf{P}_1$ will cause an additional force due to body rotation and/or the straining component $\boldsymbol{E}^\infty$ of an imposed flow. Owing to linearity, the former can only be constructed as $(\boldsymbol{\Omega}-\boldsymbol{\Omega}^\infty(\mathbf{x_p}))\times\mathbf{P}_1$, whereas the latter can only take the form of $\boldsymbol{E}^\infty\cdot\mathbf{P}_1$, as shown in (36).

In Sec. V, we will provide pictorial illustrations of how these dipole and quadrupole forces arise physically due to stick–slip asymmetry.

B. Faxen torque relation

Similarly, we can evaluate each term of (20) for the torque as follows. For the uniform-slip part, only the body rotation $(\boldsymbol{\Omega}\times\mathbf{y}-\boldsymbol{u}^\infty)$ term contributes, recovering the usual Stokes torque obtained by previous studies,[15,16]

$$\boldsymbol{T}_0 = \frac{-8\pi\mu a^3}{1+3\lambda}[\boldsymbol{\Omega}-\boldsymbol{\Omega}^\infty(\mathbf{x_p})]. \tag{37}$$

The torque exerted by the imposed flow stress, the second term in $\boldsymbol{T}_0$ in (20b), is identically zero. The derivation of (37) is standard after using (30a) and (30b) in (20b) [see (B2) and (B3)].

For the non-uniform slip part $\boldsymbol{T}'$, it has two contributions: the dipole torque $\boldsymbol{T}'_D$ and the quadrupole torque $\boldsymbol{T}'_Q$. Each contribution consists of the torque exerted by the imposed flow and the torque generated by the body movements. These torques can be evaluated as

$$\begin{aligned}\boldsymbol{T}'_D &\equiv \varepsilon a\int_{S_p} 3[\langle f\mathbf{S}_1\rangle\cdot\mathbf{S}_1]\,\mathbf{y} \\ &\quad\times\left[\boldsymbol{R}^R_{||}\cdot\left(\mathbf{y}\cdot\nabla\boldsymbol{\sigma}^\infty|_{\mathbf{x_p}}+\frac{\mathbf{yyy}}{3!}\vdots\nabla\nabla\nabla\boldsymbol{\sigma}^\infty|_{\mathbf{x_p}}+\cdots\right)\cdot\mathbf{n}\right]\mathrm{d}S \\ &\quad+\varepsilon a\mu\int_{S_p}3[\langle f\mathbf{S}_1\rangle\cdot\mathbf{S}_1]\mathbf{y}\times\left[\boldsymbol{R}^R\cdot\left(\boldsymbol{R}^T_{||}\cdot(\boldsymbol{U}-\boldsymbol{u}^\infty(\mathbf{x_p}))\right)\right]\mathrm{d}S \\ &= \frac{18\pi\mu a^2}{(1+3\lambda)^2}\mathbf{P}_1\times(\boldsymbol{U}-\boldsymbol{u}^\infty(\mathbf{x_p})) \\ &\quad-\frac{12}{5}\frac{\pi a^4}{(1+3\lambda)}\left(1+\frac{a^2}{14}\nabla^2\right)\nabla\times\boldsymbol{\sigma}^\infty|_{\mathbf{x_p}}\cdot\mathbf{P}_1,\end{aligned} \tag{38}$$

$$\begin{aligned}\boldsymbol{T}'_Q &\equiv \varepsilon a\int_{S_p}(5/6)[\langle f\mathbf{S}_2\rangle:\mathbf{S}_2] \\ &\quad\mathbf{y}\times\left[\boldsymbol{R}^R_{||}\cdot\left(\boldsymbol{\sigma}^\infty|_{\mathbf{x_p}}+\frac{\mathbf{yy}}{2!}:\nabla\nabla\boldsymbol{\sigma}^\infty|_{\mathbf{x_p}}+\cdots\right)\cdot\mathbf{n}\right]\mathrm{d}S \\ &\quad+\varepsilon a\mu\int_{S_p}(5/6)[\langle f\mathbf{S}_2\rangle:\mathbf{S}_2]\mathbf{y}\times\left[\boldsymbol{R}^R\cdot(\boldsymbol{R}^R_{||}\cdot((\boldsymbol{\Omega}-\boldsymbol{\Omega}^\infty(\mathbf{x_p}))\times\mathbf{y}))\right]\mathrm{d}S \\ &= -\frac{12\pi\mu a^2}{(1+3\lambda)}\mathbf{P}_2\cdot(\boldsymbol{\Omega}-\boldsymbol{\Omega}^\infty(\mathbf{x_p}))-\frac{8\pi\mu a^3}{(1+3\lambda)}\mathbf{P}_2 \\ &\quad\times\left(1+\frac{a^2}{14}\nabla^2\right)\boldsymbol{E}^\infty(\mathbf{x_p})-\frac{4}{7}\frac{\pi a^5}{(1+3\lambda)}\nabla\times\nabla\boldsymbol{\sigma}^\infty|_{\mathbf{x_p}}:\mathbf{P}_2.\end{aligned} \tag{39}$$

Both (38) and (39) are the results after reducing the integrals by using (30a)–(30d). How to arrive at these results in detail can be found in (B4)–(B10).

Combining (37)–(39) yields the Faxen torque relation as

$$\begin{aligned}\boldsymbol{T} &= -\frac{8\pi\mu a^3}{1+3\lambda}\left(\mathbf{I}+\frac{3/2}{1+3\lambda}\mathbf{P}_2\right)\cdot(\boldsymbol{\Omega}-\boldsymbol{\Omega}^\infty(\mathbf{x_p})) \\ &\quad+\frac{18\pi\mu a^2}{(1+3\lambda)^2}\mathbf{P}_1\times(\boldsymbol{U}-\boldsymbol{u}^\infty(\mathbf{x_p})) \\ &\quad-\frac{8\pi\mu a^3}{1+3\lambda}\mathbf{P}_2\times\left(1+\frac{a^2}{14}\nabla^2\right)\boldsymbol{E}^\infty(\mathbf{x_p}) \\ &\quad-\frac{12}{5}\frac{\pi a^4}{(1+3\lambda)}\left(1+\frac{a^2}{14}\nabla^2\right)\nabla\times\boldsymbol{\sigma}^\infty|_{\mathbf{x_p}}\cdot\mathbf{P}_1 \\ &\quad-\frac{4}{7}\frac{\pi a^5}{(1+3\lambda)}\nabla\times\nabla\boldsymbol{\sigma}^\infty|_{\mathbf{x_p}}:\mathbf{P}_2.\end{aligned} \tag{40}$$

Equation (40) reveals that $O(\varepsilon)$ non-uniform slip affects the torque in three ways: (i) body rotation via $\mathbf{P}_2$, (ii) translation coupling via $\mathbf{P}_1$, and (iii) the imposed flow via both $\mathbf{P}_1$ and $\mathbf{P}_2$. In (iii), the contributions can further involve higher order finite-size corrections if the imposed flow gradient is non-uniform. Again, if the imposed flow is linear or (35) is satisfied, we can neglect the higher order terms $a^2\nabla^2$, $\nabla\times\boldsymbol{\sigma}^\infty|_{\mathbf{x_p}}\cdot\mathbf{P}_1$ and $\nabla\times\nabla\boldsymbol{\sigma}^\infty|_{\mathbf{x_p}}:\mathbf{P}_2$ in (40). This reduces (40) to

$$\boldsymbol{T} = -\frac{8\pi\mu a^3}{1+3\lambda}\left(\mathbf{I}+\frac{3/2}{1+3\lambda}\mathbf{P}_2\right)\cdot(\boldsymbol{\Omega}-\boldsymbol{\Omega}^\infty(\mathbf{x_p})) + \frac{18\pi\mu a^2}{(1+3\lambda)^2}\mathbf{P}_1\times(\boldsymbol{U}-\boldsymbol{u}^\infty(\mathbf{x_p})) - \frac{8\pi\mu a^3}{(1+3\lambda)}\mathbf{P}_2\times\boldsymbol{E}^\infty(\mathbf{x_p}). \tag{41}$$

As indicated by (41), dipole $\mathbf{P}_1$ will contribute to a coupling torque through the translational velocity $[\boldsymbol{U}-\boldsymbol{u}^\infty(\mathbf{x_p})]$ with respect to the imposed flow. Since torque is a pseudovector, this torque can only be constructed as $\mathbf{P}_1\times(\boldsymbol{U}-\boldsymbol{u}^\infty(\mathbf{x_p}))$ through linearity. Quadrupole $\mathbf{P}_2$ will provide a correction to the Stokes torque. Similarly, this quadrupole torque can only take the form of $\mathbf{P}_2\cdot(\boldsymbol{\Omega}-\boldsymbol{\Omega}^\infty(\mathbf{x_p}))$ relative to the imposed flow vorticity. Moreover, when there is an imposed flow, an additional quadrupole torque arising from the straining component $\boldsymbol{E}^\infty$ can only be constructed as $\mathbf{P}_2\times\boldsymbol{E}^\infty$. How these torques are generated due to stick–slip asymmetry will be discussed next in Sec. V.

V. SURFACE-MOMENT FORCES AND TORQUES ARISING FROM STICK–SLIP ASYMMETRY

As displayed in (36) and (41), we have shown a variety of additional hydrodynamic forces and torques induced by surface dipole $\mathbf{P}_1$

and surface quadrupole $\mathbf{P}_2$. In this section, we provide pictorial physical explanations for how these forces and torques form due to stick-slip asymmetry. They can be generated either by body movements or exerted under the actions of imposed flows, which are discussed separately below.

A. Additional resistance forces and torques induced by surface moments

Body translation/rotation will generate a resistance force/torque to oppose the motion of a sphere. Dipole $\mathbf{P}_1$ basically creates an anti-symmetry in the forces on different faces of a non-uniform slip Janus sphere. This results in translation-rotation coupling, generating a rotation-coupling force $\zeta a\boldsymbol{\Omega} \times \mathbf{P}_1$ (in scale of $\varepsilon\mu\Omega a^2$ with $\zeta \sim \mu a$ being the drag coefficient) or a translation-coupling torque $\zeta a\mathbf{P}_1 \times \boldsymbol{U}$ (in scale of $\varepsilon\mu U a^2$). How such a force/torque form can be pictured using a two-faced stick–slip Janus sphere when it is translating/spinning in a quiescent fluid, as illustrated in Fig. 3.

First, consider the situation where the sphere is rotating at an angular velocity $\boldsymbol{\Omega}$ in a quiescent fluid. As illustrated in Fig. 3(a), the stick face will impart a more shear force on the fluid than the slip face along the spinning direction, exceeded by an order of $\varepsilon\mu\Omega a^2$ due to the slip difference ε. In other words, the stick face will receive a more drag force against the spinning motion, which, in turn, drives the sphere to migrate. Similarly, when the sphere is translating at a prescribed velocity $\boldsymbol{U}$, the drag force on the stick face will be greater than that on the slip face in a magnitude of $\varepsilon\mu U a$. This generates a couple $\varepsilon\mu U a^2$ on the sphere to make it rotate, as illustrated in Fig. 3(b).

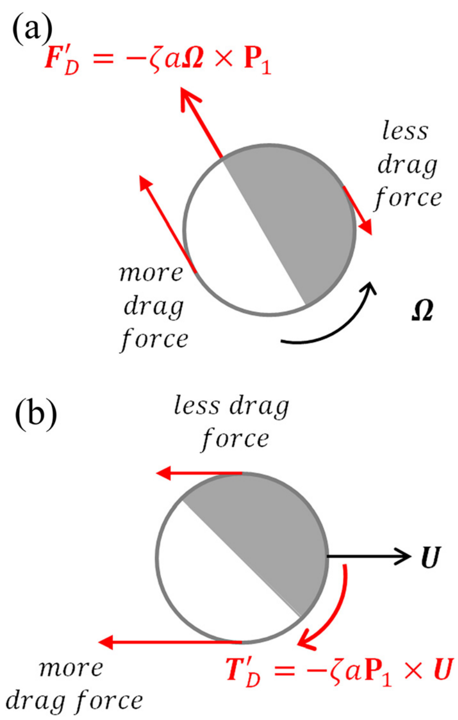

FIG. 3. Schematic illustrations of how the dipole force $\boldsymbol{F}'_D$ and torque $\boldsymbol{T}'_D$ arise due to translation-rotation coupling. (a) illustrates how a rotation-coupling force $\boldsymbol{F}'_D = -\zeta a\boldsymbol{\Omega} \times \mathbf{P}_1$ is generated onto a stick–slip sphere when it spins at an angular velocity $\boldsymbol{\Omega}$. Such a force is a result of the asymmetric shearing forces exerted on the stick and the slip faces. Similarly, if the sphere is moving at a velocity $\boldsymbol{U}$, an asymmetric drag force pair on the stick and the slip faces will produce a translation-coupling torque $\boldsymbol{T}'_D = -\zeta a\mathbf{P}_1 \times \boldsymbol{U}$ to the sphere, as illustrated in (b).

As for quadrupole $\mathbf{P}_2$, we use a symmetric slip–stick–slip Janus sphere to illustrate how $\mathbf{P}_2$ causes additional force and torque acting differently along the two axes of symmetry of the sphere. This explains the induced force $-\zeta\mathbf{P}_2 \cdot \boldsymbol{U}$ (in scale of $\varepsilon\mu U a$) and torque $-\zeta a^2\mathbf{P}_2 \cdot \boldsymbol{\Omega}$ (in scale of $\varepsilon\mu\Omega a^3$). As shown in Fig. 4(a), we first consider the case when the sphere is moving at a prescribed velocity $\boldsymbol{U}$ in a quiescent fluid. For simplicity, we assume that the sphere orients with 45° respect to $\boldsymbol{U}$ so that the poles along direction $\mathbf{d}$ and the stripe in the orthogonal direction $\mathbf{d} \cdot (\mathbf{I} - \mathbf{dd})$ will feel an equal amount of impacts from the velocity. However, due to the stick-slip asymmetry, the slip poles will experience a less drag force than the stick stripe in a magnitude of $\varepsilon\mu U a$, making the overall drag force on the sphere no longer be parallel to $-\boldsymbol{U}$. Because $\mathbf{P}_2 = \mathcal{Q}(3\mathbf{d}\,\mathbf{d} - \mathbf{I})$ according to (25b), such a quadrupole drag force can be decomposed as

$$\boldsymbol{F}'_Q \equiv -\zeta\mathbf{P}_2 \cdot \boldsymbol{U} = -2\mathcal{Q}\mathbf{dd} \cdot \zeta\boldsymbol{U} - \mathcal{Q}(\mathbf{dd} - \mathbf{I}) \cdot \zeta\boldsymbol{U}. \quad (42)$$

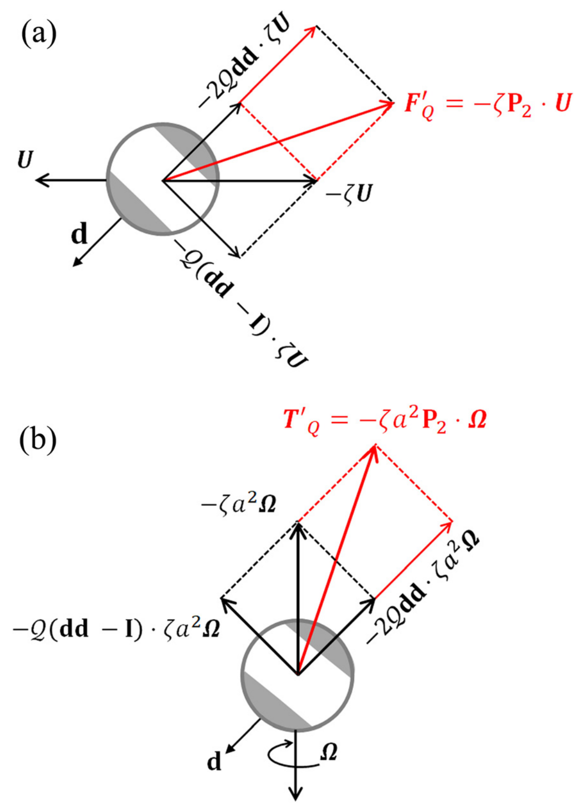

FIG. 4. Schematic illustrations of how the quadrupole force $\boldsymbol{F}'_Q$ and torque $\boldsymbol{T}'_Q$ are generated on a slip–stick–slip Janus sphere. (a) When the sphere is moving at a constant velocity $\boldsymbol{U}$, the slip poles will feel lower drag force than the stick stripe, resulting in the overall resistance force $\boldsymbol{F}'_Q = -\zeta\mathbf{P}_2 \cdot \boldsymbol{U}$ no longer parallel to $-\boldsymbol{U}$. (b) Similarly, $\boldsymbol{T}'_Q = -\zeta a^2\mathbf{P}_2 \cdot \boldsymbol{\Omega}$ can be generated in a direction dis-aligned to the rotation axis when the sphere spins at an angular velocity $\boldsymbol{\Omega}$.

Thus, in the present example, the drag force on the poles will be twice that on the stripe.

A similar picture shown in Fig. 4(b) can also be used to visualize how the quadrupole resistance torque $-\zeta a^2 \mathbf{P}_2 \cdot \mathbf{\Omega}$ is generated when the sphere rotates at an angular velocity $\mathbf{\Omega}$,

$$\boldsymbol{T}'_Q \equiv -\zeta a^2 \mathbf{P}_2 \cdot \mathbf{\Omega} = -2\mathcal{Q}\mathbf{dd} \cdot \zeta a^2 \mathbf{\Omega} - \mathcal{Q}(\mathbf{dd} - \mathbf{I}) \cdot \zeta a^2 \mathbf{\Omega}. \quad (43)$$

As indicated by (43), this torque will be dis-aligned to the principal rotation axis due to the stick–slip asymmetry.

As explained above, because of stick-slip asymmetry, these additional resistance forces and torques arising from $\mathbf{P}_1$ and $\mathbf{P}_2$ will not be acting in parallel to the prescribed velocities $\boldsymbol{U}$ and $\mathbf{\Omega}$. This means that if there is an external force or torque applied to a non-uniform slip sphere, the sphere will translate/rotate in a direction unparallel to the applied force/torque due to $\mathbf{P}_2$. In addition, because the translation and rotation are now coupled due to $\mathbf{P}_1$, the applied force may cause the sphere to rotate, whereas the applied torque may set up a translation to the sphere.

B. Surface-moment forces and torques due to imposed flow gradients: Joint stick–slip asymmetry and flow symmetry

Unlike resistance force/torque against body motion, an imposed flow will exert a propulsion force/torque on a non-uniform slip sphere to make the sphere move along with the stream. While slip anisotropy breaks symmetry in geometry, this geometrical asymmetry can join with the symmetry/anti-symmetry of an imposed flow to generate additional forces and torques. When the flow is linear, dipole $\mathbf{P}_1$ and quadrupole $\mathbf{P}_2$ can couple to the flow's symmetric straining component $\boldsymbol{E}^\infty$ to generate additional force $\zeta a \mathbf{P}_1 \cdot \boldsymbol{E}^\infty$ (in scale of $\varepsilon\mu E^\infty a^2$) and torque $\zeta a^2 \mathbf{P}_2 \times \boldsymbol{E}^\infty$ (in scale of $\varepsilon\mu E^\infty a^3$) on the sphere, as given in (36) and (41).

In Fig. 5, we use stick–slip and slip–stick–slip Janus spheres to illustrate the above effects of $\mathbf{P}_1$ and $\mathbf{P}_2$ in the presence of linear flow fields. Figure 5(a) illustrates how the dipole straining force $\zeta a \mathbf{P}_1 \cdot \boldsymbol{E}^\infty$ is generated by placing a stick–slip Janus sphere at the center of a pure straining flow. It is clear that if the sphere is not aligned to the compression axis or to the stretching axis of the flow, the sphere will experience asymmetric forces on its two faces. Specifically, the slip face will receive a less force from the applied straining flow than the stick face. Since these two forces are acting in the opposite directions, a net force will be resulted to act on the stick side of the sphere and, hence, will drive the sphere away from the flow center. Note that no torque is generated by dipole in this case since $\epsilon_{ijk} P_{1j} E^\infty_{jk}$ is identically zero because of the symmetry of E^∞_{jk}. Figure 5(b) illustrates how the quadrupole-straining torque $\zeta a^2 \mathbf{P}_2 \times \boldsymbol{E}^\infty$ is generated on a stick–slip–stick Janus sphere when it is placed at the center of a pure straining flow. In this case, a force pair of the same amount but in the opposite directions is acting on the two slip poles, so is that on the stripe portion. This anti-symmetric force pair, thus, generates a couple onto the sphere without net force.

As for the vorticity component $\mathbf{\Omega}^\infty$ of the imposed flow, it produces effects exactly like those due to the angular velocity $\mathbf{\Omega}$ of the sphere but in the opposite manner because of pushing by the flow. Similar to Figs. 3(a) and 4(b) due to $\mathbf{\Omega}$, there are additional dipole force $\zeta a \mathbf{\Omega}^\infty \times \mathbf{P}_1$ and quadrupole torque $\zeta a^2 \mathbf{\Omega}^\infty \cdot \mathbf{P}_2$ generated by $\mathbf{\Omega}^\infty$, as illustrated in Fig. 6 by having a non-uniform slip sphere held fixed at the center of a pure rotating flow field. If the sphere is freely suspended, to ensure both force and torque free, $\zeta a \mathbf{\Omega}^\infty \times \mathbf{P}_1$ must be canceled out exactly by $-\zeta a \mathbf{\Omega} \times \mathbf{P}_1$ and so be $\zeta a^2 \mathbf{\Omega}^\infty \cdot \mathbf{P}_2$ by $-\zeta a^2 \mathbf{\Omega} \cdot \mathbf{P}_2$, just like the leading order uniform slip case where the Stokes torque $\zeta a^2(\mathbf{\Omega} - \mathbf{\Omega}^\infty)$ is zero. In this case, the sphere will simply display a rigid body rotation at $\mathbf{\Omega} = \mathbf{\Omega}^\infty$, meaning that there is no impact from $\mathbf{\Omega}$ on the sphere's motion.

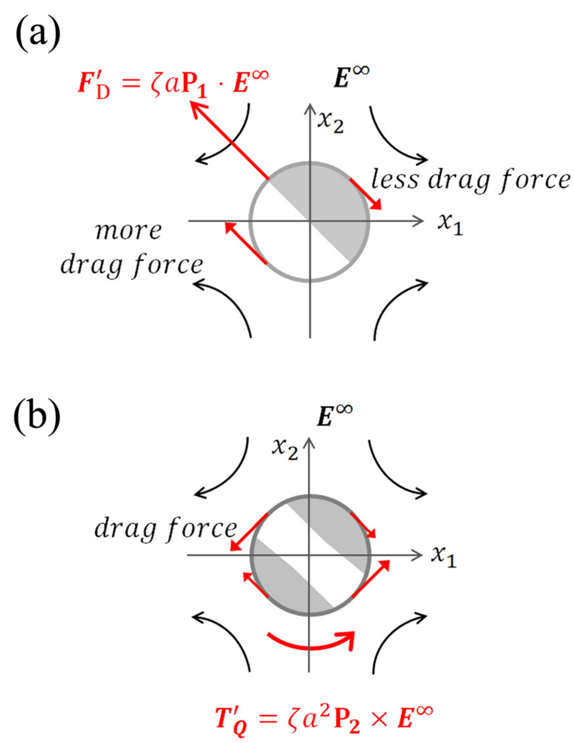

FIG. 5. Schematic illustrations of how additional force and torque arise onto a non-uniform slip Janus sphere when it is placed at the center of a pure straining flow. (a) illustrates that a two-faced stick–slip Janus sphere possessing a dipole $\mathbf{P}_1$ can experience opposite but unequal forces on the stick and the slip faces. This generates a dipole-straining force $\zeta a \mathbf{P}_1 \cdot \boldsymbol{E}^\infty$ onto the sphere, which will drive the sphere away from the flow center. (b) Similarly, a quadrupole-straining torque $\zeta a^2 \mathbf{P}_2 \times \boldsymbol{E}^\infty$ can be generated onto a symmetric slip–stick–slip Janus sphere due to the anti-symmetric force pair induced by a quadrupole $\mathbf{P}_2$.

Similar to the effects of $\mathbf{\Omega}^\infty$ as above, the imposed flow velocity $\boldsymbol{u}^\infty(\mathbf{x_p})$ can also set up surface moment force and torque of the same types as those caused by the translational velocity $\boldsymbol{U}$ of a non-uniform slip sphere. They are the dipole torque $\zeta a \mathbf{P}_1 \times \boldsymbol{u}^\infty(\mathbf{x_p})$ due to translation coupling and the quadrupole torque $\zeta \mathbf{P}_2 \cdot \boldsymbol{u}^\infty(\mathbf{x_p})$. As illustrated in Fig. 7, these torque and force are acting in the manner opposite to those set up by $\boldsymbol{U}$ [see Figs. 3(b) and 4(a)]. Thus, when the sphere is freely suspended as both force and torque on the sphere are zero, the sphere must migrate along the stream at $\boldsymbol{U} = \boldsymbol{u}^\infty(\mathbf{x_p})$, just like the leading order uniform slip case where the Stokes force $\zeta(\boldsymbol{U} - \boldsymbol{u}^\infty(\mathbf{x_p}))$ is zero.

VI. NEW IMPACTS DUE TO SURFACE-MOMENT-MEDIATED FAXEN CORRECTIONS

As shown in (36) and (41), the additional surface-moment-induced forces and torques exerted by imposed flows are the first

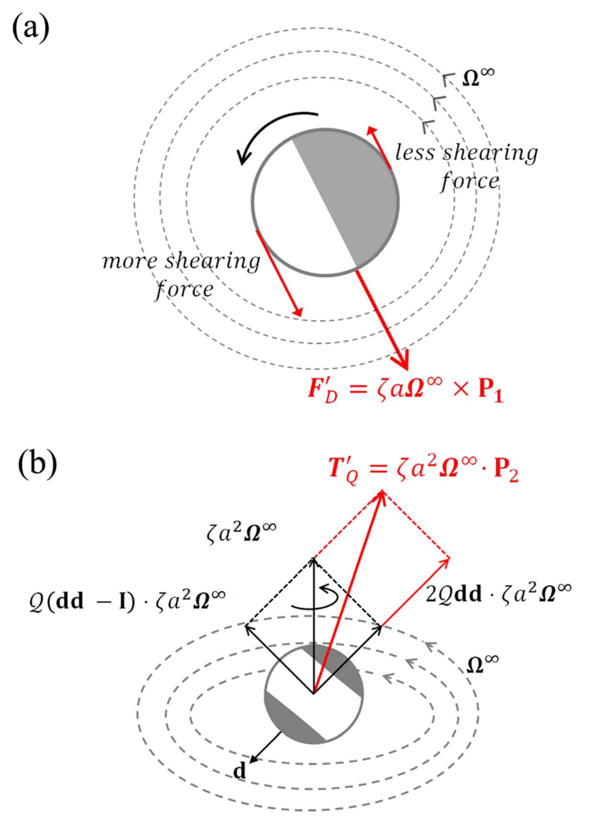

FIG. 6. Schematic illustrations of how additional force and torque arise onto a non-uniform slip Janus sphere when it is held fixed at the center of a pure rotating flow field. (a) illustrates that the flow vorticity $\boldsymbol{\Omega}^\infty$ can set up a rotation-coupling force $\zeta a \boldsymbol{\Omega}^\infty \times \mathbf{P}_1$ due to the dipole of a two-faced stick–slip sphere, similar to Fig. 3(a). (b) illustrates how an extra quadrupole torque $\zeta a^2 \boldsymbol{\Omega}^\infty \cdot \mathbf{P}_2$ is generated in a direction dis-aligned to the principal rotation axis of a symmetric slip–stick–slip Janus sphere, similar to Fig. 4(b).

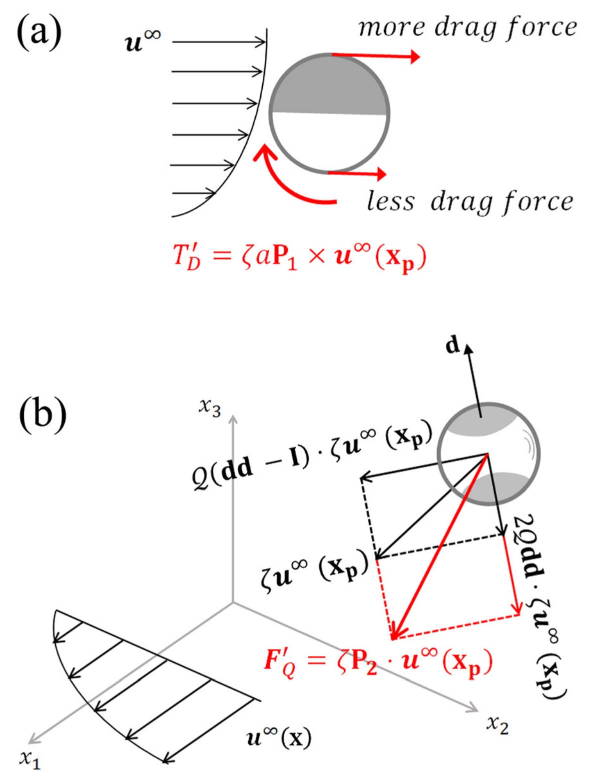

FIG. 7. Schematic illustrations of how surface-moment-induced force and torque arise onto a non-uniform slip Janus sphere that is held fixed in an arbitrary flow field $\boldsymbol{u}^\infty$. (a) illustrates how a torque $\zeta a \mathbf{P}_1 \times \boldsymbol{u}^\infty(\mathbf{x_p})$ is induced by a dipole through coupling to the imposed flow velocity $\boldsymbol{u}^\infty(\mathbf{x_p})$ at the sphere's position, similar to Fig. 3(b). (b) illustrates how a force $\zeta \mathbf{P}_2 \cdot \boldsymbol{u}^\infty(\mathbf{x_p})$ is generated by a quadrupole, similar to Fig. 4(a).

effects due to slip anisotropy based on the assumption (35) under which the standard Faxen-type finite-size corrections or non-uniform flow gradient effects are negligible so that the more general Faxen relations (34) and (40) can be reduced to the simplified forms (36) and (41). However, if the imposed flow field happens to be non-linear like a pressure-driven quadratic flow in a channel, then the more general Faxen relations (34) and (40) should be employed for better characterizing the hydrodynamic force and torque on the sphere in that situation. Such finite-size Faxen corrections may also be vital in the multi-particle situation such as a dilute suspension of stick–slip or slip–slip spheres. In this case, hydrodynamic interactions between these heterogeneous spheres need to be quantified using the method of reflections with the full Faxen relations (34) and (40). In such a situation, the background flow $\boldsymbol{u}^\infty$ around a test sphere can be taken to be the disturbance flow field generated by the surrounding spheres. The gradient of such a flow is clearly non-uniform, reflected by the terms $\boldsymbol{E}^\infty$, $\nabla\boldsymbol{\sigma}^\infty$, $\nabla\nabla\boldsymbol{\sigma}^\infty$, $\nabla\times\boldsymbol{\sigma}^\infty$, and $\nabla\times\nabla\boldsymbol{\sigma}^\infty$ working jointly with surface dipole or quadrupole. The form of these terms appears to resemble those for ellipsoid due to joint geometry and flow effects.[26] Because the effects of such surface moment terms tend to act in preferential directions either along or across the velocity gradients of the background flow, hydrodynamic interactions between non-uniform slip spheres will become anisotropic even in a uniformly distributed suspension of such spheres. Also, for this reason, the first finite-size corrections to the force on a non-uniform slip sphere due to background flow gradient effects will no longer be of the standard Faxen type under the operator $a^2\nabla^2$, but come from surface moment contributions. The latter is mainly from the dipole-straining term $\mathbf{P}_1 \cdot \boldsymbol{E}^\infty(\mathbf{x_p})$ in (34) due to the linear part of the background flow. Similarly, the quadrupole-straining term $\mathbf{P}_2 \times \boldsymbol{E}^\infty(\mathbf{x_p})$ in (40) will be the main finite-size contribution to the torque. Note that involving the rate of strain tensor $\boldsymbol{E}^\infty$ is typically associated with the symmetric force dipole, namely, stresslet, for computing the effective viscosity of a particle suspension.[27] This suggests that the force and stresslet on a non-uniform slip sphere will also be coupled and so will the torque and stresslet. Further notice that either coupling can exist alone or both co-exist, depending on whether the sphere is of two-faced type dominated by dipole, striped type dominated by quadrupole, or mixed with these two types. This means that the nature of hydrodynamic interactions between non-uniform slip spheres will depend on the type of slip pattern. In light of the above, the rheology of a suspension of such spheres is expected to differ both qualitatively and quantitatively compared to that of a suspension of no-slip or uniform slip spheres.

VII. PERSPECTIVES AND OUTLOOKS

We have developed a theory capable of unraveling essential hydrodynamic features for non-uniform slip spheres. The main idea is that an uneven slip length distribution will render an asymmetric force distribution over the surface of a non-uniform slip sphere because of symmetry breaking. This will induce additional hydrodynamic forces/torques on the sphere, depending on how the slip length varies spatially along the sphere's surface.

The theory is built upon a new and more generalized framework formulated by the reciprocal theorem in conjunction with surface harmonic expansion, allowing us to derive a new set of the Faxen formulas for the hydrodynamic force and torque on a weakly non-uniform slip sphere with an arbitrary slip length distribution. With the aid of these formulas, we are able to codify various forces and torques arising from slip anisotropy—all can be interpreted in terms of surface dipole and quadrupole, corresponding to antisymmetric stick-slip-like and symmetric slip-stick-slip-like distributions, respectively.

One might think that a non-uniform slip Janus sphere may act hydrodynamically like a spheroid or a rod-like particle. It seems that such an analogy holds only when the sphere is of striped or slip-stick-slip type dominated by quadrupole, but not for two-faced stick-slip type dictated by dipole. The reason for this is that quadrupole preserves geometrical symmetry in terms of the two principal axes of body revolution. Specifically, the drag forces on different parts of the sphere's surface can still display a spatial symmetry with respect to the two principal axes of revolution. On the other hand, dipole breaks geometrical symmetry in one particular direction, which often gives rise to an unequal drag force pair when the applied force is not aligned to that direction. It is this reason why dipole can give rise to coupling between force and rotation as well as a coupling between torque and translation. Such dipole-induced hydrodynamic coupling becomes more manifested in the presence of imposed flows. For a dipolar sphere like a two-faced stick–slip sphere, dipole can be coupled to the straining component of the imposed flow field to produce an asymmetric force, which will make the sphere drift across the streamlines.

Quadrupole, on the other hand, typically dominates in the motion of a slip–stick–slip or stripe-like sphere. It mainly produces a drag force in plane with the director and translational velocity $\boldsymbol{U}$ of the sphere, pointing in a direction unparallel to $-\boldsymbol{U}$. Similarly, an additional torque can also be introduced by quadrupole. This torque is acting in plane with the director and angular velocity $\boldsymbol{\Omega}$ of the sphere, making the overall torque dis-aligned to the principal axis of rotation. When there is an imposed flow, the same quadrupole torque, but in the opposite direction, can also arise from the vorticity component of the flow, $\boldsymbol{\Omega}^{\infty}$. If the sphere is freely suspended, these two oppositely acting quadrupole torques of the same type will exactly cancel out like the equal but adverse Stokes torques generated by $\boldsymbol{\Omega}$ and $\boldsymbol{\Omega}^{\infty}$ in the uniform slip case, leading the sphere to rotate at $\boldsymbol{\Omega} = \boldsymbol{\Omega}^{\infty}$ [up to $O(\varepsilon)$]. In other words, except for trivial rigid body rotation, there is no impact from $\boldsymbol{\Omega}^{\infty}$ [up to $O(\varepsilon)$] on the motion of the sphere due to quadrupole under the freely suspended situation.

In view of the above, given that the effects of surface dipole and quadrupole are rather distinct, it is possible to make use of their characteristic differences to tell which one dominates the surface pattern of a non-uniform slip Janus sphere. That is, one can utilize the hydrodynamic features of dipole and quadrupole to tell whether a Janus sphere belongs to two-faced or striped type. For instance, to see whether the sphere is of two-faced type characterized by dipole, one can place the sphere at the center of a pure straining field (of $\boldsymbol{E}^{\infty}$) to see if the sphere can undergo spinning due to the quadrupole-straining torque [the $\mathbf{P}_2 \times \boldsymbol{E}^{\infty}$ term in (41)] or exhibit drifting across the streamlines due to the dipole-straining force [the $\mathbf{P}_1 \cdot \boldsymbol{E}^{\infty}$ term in (36)]. To identify whether the sphere is of striped type controlled by quadrupole, perhaps it can be achieved by placing the sphere in a simple shear flow and by observing if its rotation dynamics display Jeffery orbits like those of a spheroid [due to the $\mathbf{P}_2 \times \boldsymbol{E}^{\infty}$ term in (41)]. In any case, the dynamics of a non-uniform slip sphere should reveal some insights into how dipole or quadrupole plays a role. In particular, by observing how non-uniform spheres respond to various applied forcing or flow conditions, one might be able to utilize these responses to characterize or sort the spheres hydrodynamically. All these aspects can be tested experimentally using microfluidic devices. But prior to performing such an experiment, it is necessary to analyze how a non-uniform slip sphere behaves in its motion, depending on the specific forcing or flow condition applied. This requires applying the new Faxen force and torque relations (36) and (41) to determine both the translational and rotational dynamics of the sphere. Solving such mobility problems is of particular interest for the swimming of a squirmer self-propelled by a prescribed slip velocity on its surface.[4,5] Along this line, it will be interesting to look at the situation where a squirmer possesses both stick and slip portions on its surface. For such a heterogeneous squirmer, its swimming velocity is expected to be sensitive to the stick–slip partition, which can be readily described by the new framework given in the present study.

Finally, the full Faxen relations (34) and (40) with surface moment contributions should modify effects at play in systems involving more than one non-uniform slip spheres, especially on the nature of hydrodynamic interactions between such spheres. This is rooted in the fact that these surface moment contributions to a test sphere tend to act in preferential directions along or across the velocity gradients of the background flow generated by the surrounding spheres. The effects would become much more pronounced in a suspension of non-uniform slip spheres. The reason is that even if these spheres are uniformly distributed, hydrodynamic interactions between them could become anisotropic because of preferential polarity effects of surface moments. This may alter not only the collective nature of hydrodynamic interactions but also the microstructure of such suspension. For this reason, the rheological properties of such suspension are expected to be distinct from those of a suspension of no-slip or uniform slip spheres. Studying suspension hydrodynamics of this sort will be the next topic requiring more investigations. The present work at least provides some foundations for future pursuit of such a study.

ACKNOWLEDGMENTS

This work was supported by the Ministry of Science and Technology of Taiwan under Grant Nos. MOST 109-2811-E-006-508 and 110-2811-E-006-507.

AUTHOR DECLARATIONS

Conflict of Interest

The authors have no conflicts to disclose.

DATA AVAILABILITY

The data that support the findings of this study are available within the article.

APPENDIX A: DERIVATION OF THE FAXEN FORCE RELATION (34)

To compute the force using (19), we need the following resistance tensors according to (15):

$$R_{ij}^{T} = \mathscr{A}\delta_{ij} + \mathscr{B}n_i n_j, \tag{A1a}$$

$$R_{ij||}^{T} = \mathscr{A}\left(\delta_{ij} - n_i n_j\right), \tag{A1b}$$

$$R_{ij}^{R} = \mathscr{C}\delta_{ij}, \tag{A1c}$$

$$R_{ij||}^{R} = \mathscr{C}\left(\delta_{ij} - n_i n_j\right), \tag{A1d}$$

where $\mathscr{A} = -3/[2a(1+3\lambda)]$, $\mathscr{B} = -18\lambda/[2a(1+3\lambda)]$, and $\mathscr{C} = -3/[a(1+3\lambda)]$.

The force (19) consists of the uniform-slip part $\boldsymbol{F}_0$ and the non-uniform slip part $\boldsymbol{F}'$,

$$\boldsymbol{F} = \boldsymbol{F}_0 + \boldsymbol{F}', \tag{A2a}$$

$$\boldsymbol{F}_0 = \mu\int_{S_p}\left(U_j - u_j^{\infty}\right)R_{ij}^{T}\,dS + a\lambda\int_{S_p} R_{ij||}^{T}\,\sigma_{jk}^{\infty}\,n_k\,dS, \tag{A2b}$$

$$\begin{aligned}\boldsymbol{F}' &= \varepsilon a\int_{S_p} f(\mathbf{y})\,R_{ij||}^{T}\,\sigma_{jk}^{\infty}\,n_k\,dS \\ &\quad + \varepsilon a\mu\int_{S_p} f(\mathbf{y})\,R_{ij}^{T}\,R_{jk||}^{R}\,\varepsilon_{kmn}\left(\Omega_m - \Omega_m^{\infty}(\mathbf{x_p})\right)y_n\,dS \\ &\quad + \varepsilon a\mu\int_{S_p} f(\mathbf{y})\,R_{ij}^{T}\,R_{jk||}^{T}\left(U_k - u_k^{\infty}(\mathbf{x_p})\right)dS.\end{aligned} \tag{A2c}$$

1. Uniform slip part F_0

As indicted by (A2b), this part is made of two terms: the body translation $(\boldsymbol{U} - \boldsymbol{u}^{\infty})$ term and the term due to the imposed flow stress $\boldsymbol{\sigma}^{\infty}$. The former can be evaluated by expanding $\boldsymbol{u}^{\infty}$ as (29a) in which only the even terms contributes. The integral can be evaluated with (A1a), (30a), and (30b), giving

$$\begin{aligned}&\mu\int_{S_p}(U_j - u_j^{\infty})R_{ij}^{T}\,dS \\ &= \mu\int_{Sp}\left[U_j - \left(u_j^{\infty}(\mathbf{x_p}) + \frac{y_p y_q}{2!}\nabla_p\nabla_q u_j^{\infty}|_{\mathbf{x_p}} + \cdots\right)\right](\mathscr{A}\delta_{ij} + \mathscr{B}n_i n_j)dS \\ &= \pi\mu a^2\left[4\mathscr{A}U_i + \frac{4}{3}\mathscr{B}U_i - 4\mathscr{A}u_i^{\infty}(\mathbf{x_p}) - \frac{4}{3}\mathscr{B}u_i^{\infty}(\mathbf{x_p})\right. \\ &\quad \left. - \frac{a^2}{2}\left(\frac{4}{3}\mathscr{A}\nabla^2 u_i^{\infty}|_{\mathbf{x_p}} + \frac{4}{15}\mathscr{B}A_{ijpq}\nabla_p\nabla_q u_j^{\infty}|_{\mathbf{x_p}}\right)\right] \\ &= -6\pi\mu a\frac{1+2\lambda}{1+3\lambda}\left[U_i - \left(1 + \frac{a^2}{6(1+2\lambda)}\nabla^2\right)\right]u_i^{\infty}(\mathbf{x_p}) \\ &\quad + \frac{6}{5}\pi\mu a^3\left(\frac{\lambda}{1+3\lambda}\right)\nabla^2 u_i^{\infty}|_{\mathbf{x_p}}.\end{aligned} \tag{A3}$$

For deriving Eq. (A3), in the terms of $A_{ijpq}\nabla_p\nabla_q u_j^{\infty}$, $(\delta_{ip}\delta_{jq} + \delta_{iq}\delta_{jp})\nabla_p\nabla_q u_j^{\infty}$ are identically zero because of the continuity $\nabla_i u_i^{\infty} = 0$. The terms higher than the quadratic terms in (29a) will not make any contributions because $\nabla^4 u_i^{\infty} = 0$.

For the imposed flow stress term, we expand $\boldsymbol{\sigma}^{\infty}$ as (29b) and find that only the odd terms contribute. With (A1b), (30a), and (30b), the integral can be evaluated as

$$\begin{aligned}&a\lambda\int_{S_p} R_{ij||}^{T}\sigma_{jk}^{\infty}\,n_k dS \\ &= a\lambda\int_{Sp}\mathscr{A}\left(\delta_{ij} - n_i n_j\right)\left(y_m\nabla_m\sigma_{jk}^{\infty}|_{\mathbf{x_p}} + \cdots\right)n_k dS \\ &= \pi a^4\lambda\mathscr{A}\left[\frac{4}{3}\delta_{ij}\delta_{km}\nabla_m\sigma_{jk}^{\infty}|_{\mathbf{x_p}} - \frac{4}{15}A_{ijkm}\nabla_m\sigma_{jk}^{\infty}|_{\mathbf{x_p}}\right] \\ &= -\frac{4}{15}\pi a^4\lambda\mathscr{A}\,\nabla_i\sigma_{jj}^{\infty}|_{\mathbf{x_p}} \\ &= -\frac{6}{5}\pi\mu a^3\left(\frac{\lambda}{1+3\lambda}\right)\nabla^2 u_i^{\infty}|_{\mathbf{x_p}}.\end{aligned} \tag{A4}$$

For deriving Eq. (A4), we have used the fact that $\delta_{ij}\delta_{km}\;\nabla_m\sigma_{jk}^{\infty}|_{\mathbf{x_p}}$ and $(\delta_{ij}\delta_{mk} + \delta_{ik}\delta_{jm})\nabla_m\sigma_{jk}^{\infty}|_{\mathbf{x_p}}$ in the $A_{ijkm}\nabla_m\sigma_{jk}^{\infty}|_{\mathbf{x_p}}$ term are identically zero because of $\nabla_k\sigma_{jk}^{\infty} = 0$. We have also used $\nabla\sigma_{jj}^{\infty} = -3\nabla p^{\infty}$, $\nabla_j\sigma_{ij}^{\infty} = 0$, and $\nabla_j\sigma_{ij}^{\infty} + \nabla_i p^{\infty} = \mu\nabla^2 u_i^{\infty}$ to simplify the results.

Combining (A3) and (A4) gives (31).

2. Non-uniform slip part F'

The force arising from slip anisotropy $\boldsymbol{F}'$ constitutes dipole force $\boldsymbol{F}'_D$ and quadrupole force $\boldsymbol{F}'_Q$. Each contribution is evaluated separately by substituting (23) into (19).

a. Dipole force F'_D

The dipole force has two contributions,

$$\boldsymbol{F}'_D \equiv \boldsymbol{F}'_{D1} + \boldsymbol{F}'_{D2}, \tag{A5a}$$

$$\boldsymbol{F}'_{D1} = \varepsilon a\int_{S_p} f(\mathbf{y})\,R_{ij||}^{T}\,\sigma_{jk}^{\infty}\,n_k\,dS, \tag{A5b}$$

$$\boldsymbol{F}'_{D2} = \varepsilon a\mu\int_{S_p} f(\mathbf{y})\,R_{ij}^{T}\,R_{jk||}^{R}\,\varepsilon_{kmn}(\Omega_m - \Omega_m^{\infty}(\mathbf{x_p}))y_n\,dS. \tag{A5c}$$

$\boldsymbol{F}'_{D1}$ is the force exerted by the imposed flow stress, while $\boldsymbol{F}'_{D2}$ is the force generated by rotation coupling. For the former, we take an expansion (29b) for $\boldsymbol{\sigma}^{\infty}$ and identify that only the even terms contribute. With (A1b) and (30a)–(30c), we can evaluate (A5b) as

$$\begin{aligned}\boldsymbol{F}'_{D1} &= \varepsilon a\int_{S_p} 3\langle f\mathrm{S}_{1m}\rangle\mathrm{S}_{1m}\,\mathscr{A}\left(\delta_{ij} - n_i n_j\right) \\ &\quad\times\left(\sigma_{jk}^{\infty}(\mathbf{x_p}) + \frac{y_p y_q}{2!}\nabla_p\nabla_q\sigma_{jk}^{\infty}|_{\mathbf{x_p}} + \cdots\right)n_k\,dS \\ &= -3\pi a^3\mathscr{A}\varepsilon\langle f\mathrm{S}_{1m}\rangle\left[\sigma_{jk}^{\infty}(\mathbf{x_p})\left(\frac{4}{3}\delta_{ij}\delta_{km} - \frac{4}{15}A_{ijkm}\right)\right. \\ &\quad\left. + \frac{a^2}{2}\nabla_p\nabla_q\sigma_{jk}^{\infty}|_{\mathbf{x_p}}\left(\frac{4}{15}A_{pqkm}\delta_{ij} - \frac{4}{105}B_{ijkmpq}\right)\right] \\ &= -3\pi a^3\mathscr{A}\varepsilon\langle f\mathrm{S}_{1m}\rangle\left[\frac{4}{5}\left(\sigma_{im}^{\infty} + \delta_{im}p^{\infty}\right)_{\mathbf{x_p}} + \frac{2}{15}a^2\nabla^2\sigma_{im}^{\infty}|_{\mathbf{x_p}}\right. \\ &\quad\left. - \frac{4}{105}a^2\left(\nabla^2\sigma_{im}^{\infty}|_{\mathbf{x_p}} + \nabla_i\nabla_m\sigma_{jj}^{\infty}|_{\mathbf{x_p}}\right)\right].\end{aligned} \tag{A6}$$

For deriving Eq. (A6), we have used $\mathrm{S}_{1m} = -n_m$ and $\sigma_{jj}^{\infty} = -3p^{\infty}$. The term $(\delta_{mp}\delta_{kq} + \delta_{kp}\delta_{mq})\nabla_p\nabla_q\sigma_{jk}^{\infty}|_{\mathbf{x_p}}$ in $A_{pqkm}\nabla_p\nabla_q\sigma_{jk}^{\infty}|_{\mathbf{x_p}}$ and the term $(\delta_{jp}A_{ikmq} + \delta_{jq}A_{ikmp})\,\nabla_p\nabla_q\sigma^\infty_{jk}|_{\mathbf{x_p}}$ in $B_{ijkmpq}\nabla_p\nabla_q\sigma^\infty_{jk}|_{\mathbf{x_p}}$ are identically zero because of $\nabla_j\sigma^\infty_{ij} = 0$. Also, in $B_{ijkmpq}\nabla_p\nabla_q\sigma^\infty_{jk}|_{\mathbf{x_p}}$, the term $\delta_{pq}\delta_{im}\delta_{jk}\nabla_p\nabla_q\sigma^\infty_{jk}|_{\mathbf{x_p}}$ in $\delta_{pq}A_{ijkm}\nabla_p\nabla_q\sigma^\infty_{jk}|_{\mathbf{x_p}}$ is zero because of $\nabla^2 p^\infty = 0$. Using $\sigma^\infty_{ij} + \delta_{ij}p^\infty = 2\mu E^\infty_{ij}$ and $\nabla^2\sigma^\infty_{ij} = 2\mu\nabla^2 E^\infty_{ij}$ in terms of the strain tensor $E^\infty_{ij} \equiv (1/2)(\nabla_i u^\infty_j + \nabla_j u^\infty_i)$, we reduce (A6) to

$$\boldsymbol{F}'_{D1} = \frac{36}{5}\frac{\pi\mu a^2}{1+3\lambda}\left(1 + \frac{5a^2}{42}\nabla^2\right)E^\infty_{ij}(\mathbf{x_p})\varepsilon\langle f S_{1j}\rangle - \frac{6}{35}\frac{\pi a^4}{1+3\lambda}\nabla_i\nabla_k\sigma^\infty_{jj}|_{\mathbf{x_p}}\varepsilon\langle f S_{1k}\rangle. \tag{A7}$$

As for $\boldsymbol{F}'_{D2}$ given by (A5c), we evaluate it using (A1a), (A1d), (30a), and (30b), yielding

$$\begin{aligned}\boldsymbol{F}'_{D2} &= \varepsilon a\mu\int_{S_p} 3\langle f S_{1p}\rangle S_{1p}\left(\mathscr{A}\delta_{ij} + \mathscr{B}n_i n_j\right) \times \mathscr{C}\left(\delta_{jk} - n_j n_k\right)\varepsilon_{kmn}(\Omega_m - \Omega^\infty_m(\mathbf{x_p}))y_n\,dS\\ &= -3\mu\pi a^4\mathscr{A}\mathscr{C}\varepsilon\langle f S_{1p}\rangle\left[\frac{4}{3}\delta_{pn}\delta_{ik} - \frac{4}{15}A_{pink}\right]\varepsilon_{kmn}(\Omega_m - \Omega^\infty_m(\mathbf{x_p}))\\ &= -\frac{18\pi\mu a^2}{(1+3\lambda)^2}\varepsilon_{imp}(\Omega_m - \Omega^\infty_m(\mathbf{x_p}))\,\varepsilon\langle f S_{1p}\rangle.\end{aligned} \tag{A8}$$

Combining (A7) and (A8), we write the final result in terms of $\mathbf{P}_1 \equiv -\varepsilon\langle f\mathbf{S}_1\rangle$, as given by (32).

b. Quadrupole force F'_Q

The quadrupole force $\boldsymbol{F}'_Q$ also has two contributions,

$$\boldsymbol{F}'_Q \equiv \boldsymbol{F}'_{Q1} + \boldsymbol{F}'_{Q2}, \tag{A9a}$$

$$\boldsymbol{F}'_{Q1} = \varepsilon a\int_{S_p} f(\mathbf{y})\,R^T_{ij||}\,\sigma^\infty_{jk}\,n_k\,dS, \tag{A9b}$$

$$\boldsymbol{F}'_{Q2} = \varepsilon a\mu\int_{S_p} f(\mathbf{y})\,R^T_{ij}\,R^T_{jk||}\,(U_k - u^\infty_k(\mathbf{x_p}))\,dS. \tag{A9c}$$

$\boldsymbol{F}'_{Q1}$ is the force exerted by the imposed flow stress, while $\boldsymbol{F}'_{Q2}$ is the force arising from body translation. To evaluate $\boldsymbol{F}'_{Q1}$, we expand $\boldsymbol{\sigma}^\infty$ as (29b) by knowing that only the odd terms contribute. Recognizing that $S_{2pq} = 3n_p n_q - \delta_{pq}$ and making use of (A1b), (30a), (30b), and $\varepsilon\langle f S_{2pq}\rangle\delta_{pq} = 0$, (A9b) can be evaluated as

$$\begin{aligned}\boldsymbol{F}'_{Q1} &= \varepsilon(5/6)a\int_{S_p}\langle f S_{2pq}\rangle S_{2pq}\mathscr{A}\left(\delta_{ij} - n_i n_j\right) \times\left(y_s\nabla_s\sigma^\infty_{jk}|_{\mathbf{x_p}} + \frac{y_m y_n y_l}{3!}\nabla_m\nabla_n\nabla_l\sigma^\infty_{jk}|_{\mathbf{x_p}} + \cdots\right)n_k\,dS\\ &= \frac{5}{2}\pi a^3\mathscr{A}\varepsilon\langle f S_{2pq}\rangle\left[a\nabla_s\sigma^\infty_{jk}|_{\mathbf{x_p}}\left(\frac{4}{15}A_{pqks}\delta_{ij} - \frac{4}{105}B_{pqijks}\right) + \frac{a^3}{6}\nabla_m\nabla_n\nabla_l\sigma^\infty_{jk}|_{\mathbf{x_p}}\left(\frac{4}{105}B_{kpqmnl}\delta_{ij} - \frac{4}{945}C_{pqijmnlk}\right)\right].\end{aligned} \tag{A10}$$

With $\nabla_j\sigma^\infty_{ij} = 0$, (A10) reduces to

$$\begin{aligned}\boldsymbol{F}'_{Q1} &= \frac{4}{21}\pi a^4\mathscr{A}\varepsilon\langle f S_{2pq}\rangle(5\nabla_p\sigma^\infty_{iq}|_{\mathbf{x_p}} - \nabla_i\sigma^\infty_{pq}|_{\mathbf{x_p}} - \delta_{ip}\nabla_q\sigma^\infty_{jj}|_{\mathbf{x_p}})\\ &\quad - \frac{2}{189}\pi a^6\mathscr{A}\varepsilon\langle f S_{2pq}\rangle(\nabla_i\nabla^2\sigma^\infty_{pq}|_{\mathbf{x_p}} + \nabla_i\nabla_p\nabla_q\sigma^\infty_{jj}|_{\mathbf{x_p}} + \delta_{ip}\nabla_q\nabla^2\sigma^\infty_{jj}|_{\mathbf{x_p}}) + \frac{2}{27}\pi a^6\mathscr{A}\varepsilon\langle f S_{2pq}\rangle\nabla^2_p\sigma^\infty_{iq}|_{\mathbf{x_p}}.\end{aligned} \tag{A11}$$

In Eq. (A11), $\nabla_q\nabla^2\sigma^\infty_{jj}|_{\mathbf{x_p}} = -3\nabla_q\nabla^2 p^\infty|_{\mathbf{x_p}} = 0$ and $\nabla_i\nabla_p\nabla_q\sigma^\infty_{jj}|_{\mathbf{x_p}} = -3\nabla_i\nabla_p\nabla_q p^\infty|_{\mathbf{x_p}} = 0$. Similarly, it can also be shown that even higher derivative terms in (29b) make no contributions at all. Therefore, (A11) becomes

$$\begin{aligned}\boldsymbol{F}'_{Q1} &= -\frac{10}{7}\frac{\pi a^3}{(1+3\lambda)}\left(1 + \frac{7a^2}{90}\nabla^2\right)\nabla_p\sigma^\infty_{iq}|_{\mathbf{x_p}}\varepsilon\langle f S_{2pq}\rangle\\ &\quad + \frac{2}{7}\frac{\pi a^3}{(1+3\lambda)}\left(1 + \frac{a^2}{18}\nabla^2\right)\nabla_i\sigma^\infty_{jq}|_{\mathbf{x_p}}\varepsilon\langle f S_{2jq}\rangle\\ &\quad + \frac{2}{7}\frac{\pi a^3}{(1+3\lambda)}\nabla_q\sigma^\infty_{jj}|_{\mathbf{x_p}}\varepsilon\langle f S_{2iq}\rangle.\end{aligned} \tag{A12}$$

For $\boldsymbol{F}'_{Q2}$ given by (A9c), it can be computed using (A1a), (A1b), (30a), and (30b), which gives

$$\begin{aligned}\boldsymbol{F}'_{Q2} &= (5/6)a\int_{S_p}\varepsilon\langle f S_{2pq}\rangle S_{pq}\left(\mathscr{A}\delta_{ij} + \mathscr{B}n_i n_j\right) \times\mathscr{A}\left(\delta_{jk} - n_j n_k\right)(U_k - u^\infty_k(\mathbf{x_p}))dS\\ &= \frac{5a}{6}\mathscr{A}^2\varepsilon\langle f S_{2pq}\rangle,\end{aligned}$$

$$\begin{aligned}&\int_{S_p}(3n_p n_q - \delta_{pq})(\delta_{ik} - n_i n_k)(U_k - u^\infty_k(\mathbf{x_p}))dS\\ &= \frac{5\pi a^3}{2}\mathscr{A}^2\varepsilon\langle f S_{2pq}\rangle(U_k - u^\infty_k(\mathbf{x_p}))\left(\frac{4}{3}\delta_{pq}\delta_{ik} - \frac{4}{15}A_{pqik}\right)\\ &= -\frac{3\pi\mu a}{(1+3\lambda)^2}\varepsilon\langle f S_{2ik}\rangle(U_k - u^\infty_k(\mathbf{x_p})).\end{aligned} \tag{A13}$$

For deriving Eq. (A13), we have used $\varepsilon\langle f S_{2pq}\rangle\delta_{pq} = 0$.

Combining (A12) and (A13) and writing the final result in terms of $\mathbf{P}_2 \equiv \varepsilon\langle f\mathbf{S}_2\rangle$, we can finally arrive at (33).

APPENDIX B: DERIVATION OF THE FAXEN TORQUE RELATION (40)

Likewise, to determine the torque using (20), we also need the resistance tensors given in (A1a)–(A1d). The torque (20) consists of the uniform slip part $\boldsymbol{T}_0$ and the non-uniform slip part $\boldsymbol{T}'$,

$$\boldsymbol{T} = \boldsymbol{T}_0 + \boldsymbol{T}', \tag{B1a}$$

$$\boldsymbol{T}_0 = \int_{S_p}\varepsilon_{ijk}\,y_j\,R^R_{kl}\left(\varepsilon_{lmn}\,\Omega_m y_n - u^\infty_l\right)dS + a\lambda\int_{S_p}\varepsilon_{imj}\,y_m\,R^R_{jk||}\,\sigma^\infty_{kp}n_p\,dS, \tag{B1b}$$

$$\begin{aligned}\boldsymbol{T}' &= \varepsilon a\int_{S_p} f(\mathbf{y})\,\varepsilon_{imj}\,y_m\,R^R_{jk||}\,\sigma^\infty_{kn}n_n\,dS\\ &\quad + \varepsilon a\mu\int_{S_p} f(\mathbf{y})\,\varepsilon_{ijk}\,y_j\,R^R_{kl}\,R^T_{lm||}(U_m - u^\infty_m(\mathbf{x_p}))\,dS\\ &\quad + \varepsilon a\mu\int_{S_p} f(\mathbf{y})\,\varepsilon_{ijk}\,y_j\,R^R_{kl}\,R^R_{lm||}\,\varepsilon_{mpq}(\Omega_p - \Omega^\infty_p(\mathbf{x_p}))y_q\,dS.\end{aligned} \tag{B1c}$$

The two contributions are evaluated separately below.

1. Uniform slip part T_0

According to (B1b), $\boldsymbol{T}_0$ is made of the body rotation term $(\Omega \times \mathbf{y} - \boldsymbol{u}^\infty)$ and the term from the imposed flow stress $\boldsymbol{\sigma}^\infty$. For the former, we expand $\boldsymbol{u}^\infty$ as (29a) in which only odd terms will contribute. With (A1c), (30a), and (30b), the integral can be evaluated as

$$\begin{aligned}&\int_{S_p} \varepsilon_{ijk} y_j R^R_{kl}\left(\varepsilon_{lmn}\Omega_m y_n - u^\infty_l\right)\mathrm{d}S\\ &= a\int_{S_p} \varepsilon_{ijk}\, y_j\, \mathscr{C}\delta_{kl}\left[\varepsilon_{lmn}\Omega_m y_n - \left(y_p\nabla_p u^\infty_l(\mathbf{x_p}) + \cdots\right)\right]\mathrm{d}S\\ &= \frac{4}{3}\pi a^4 \mathscr{C}\,\delta_{jn}\,\varepsilon_{ijk}\,\varepsilon_{mnk}\,\Omega_m - \frac{4}{3}\pi a^4\mathscr{C}\,\delta_{jp}\,\varepsilon_{ijm}\,\nabla_p u^\infty_m|_{\mathbf{x_p}}\\ &= \frac{8}{3}\pi a^4\mathscr{C}\,\Omega_i - \frac{4}{3}\pi a^4\mathscr{C}\,\varepsilon_{ijk}\,\nabla_j u^\infty_k|_{\mathbf{x_p}}\\ &= -\frac{8\pi\mu a^3}{1+3\lambda}\left[\boldsymbol{\Omega} - \boldsymbol{\Omega}^\infty(\mathbf{x_p})\right]. \end{aligned} \tag{B2}$$

For deriving Eq. (B2), we have used $\varepsilon_{ijk}\varepsilon_{mnk} = \delta_{im}\delta_{jn} - \delta_{in}\delta_{jm}$. Also recognizing that $\varepsilon_{ijk}\nabla_j u^\infty_k = 2\Omega^\infty_i$ is the vorticity of the imposed flow.

The imposed flow stress term in (B1b) is evaluated by expanding $\boldsymbol{\sigma}^\infty$ as (29b) where only even terms contribute. By using (A1c) and (30a)–(30c), the integral is found to be

$$\begin{aligned}&a\lambda\int_{S_p} \varepsilon_{imj} y_m R^R_{jk||}\,\sigma^\infty_{kn} n_n \mathrm{d}S\\ &= a^2\lambda\mathscr{C}\int_{S_p} \varepsilon_{imj} n_m\left(\delta_{jk} - n_j n_k\right)\left[\sigma^\infty_{kn}(\mathrm{x_p}) + \frac{y_p y_q}{2!}\nabla_p\nabla_q\sigma^\infty_{kn}|_{\mathrm{x_p}} + \cdots\right] n_n\mathrm{d}S\\ &= \pi a^4\lambda\mathscr{C}\varepsilon_{imj}\left[\sigma^\infty_{kn}(\mathbf{x_p})\left(\frac{4}{3}\delta_{jk}\delta_{mn} - \frac{4}{15}A_{mnjk}\right)\right.\\ &\left.+\frac{a^2}{2}\nabla_p\nabla_q\sigma^\infty_{kn}|_{\mathrm{x_p}}\left(\frac{4}{15}A_{pqmn}\delta_{jk} - \frac{4}{105}B_{pqmnjk}\right)\right]. \end{aligned} \tag{B3}$$

Because of $\nabla_j\sigma^\infty_{ij} = 0$ and $\varepsilon_{ijk}\sigma^\infty_{jk} = 0$, (B3) is identically zero.

Combining (B2) and (B3) gives (37).

2. Non-uniform slip part T'

Slip anisotropy induces dipole torque $\boldsymbol{T}'_D$ and quadrupole torque $\boldsymbol{T}'_Q$. We evaluate each separately below.

a. Dipole torque T'_D

The dipole torque $\boldsymbol{T}'_D$ is made of two contributions,

$$\boldsymbol{T}'_D \equiv \boldsymbol{T}'_{D1} + \boldsymbol{T}'_{D2}, \tag{B4a}$$

$$\boldsymbol{T}'_{D1} = \varepsilon a\int_{S_p} f(\mathbf{y})\,\varepsilon_{imj}\,y_m\,R^R_{jk||}\,\sigma^\infty_{kn}\,n_n\;\mathrm{d}S, \tag{B4b}$$

$$\boldsymbol{T}'_{D2} = \varepsilon a\mu\int_{S_p} f(\mathbf{y})\,\varepsilon_{ijk}\,y_j\,R^R_{kl}\,R^T_{lm||}\left(U_m - u^\infty_m(\mathbf{x_p})\right)\mathrm{d}S. \tag{B4c}$$

$\boldsymbol{T}'_{D1}$ is the torque exerted by the imposed flow stress, whereas $\boldsymbol{T}'_{D2}$ is the torque generated by coupling to translation. For the former given by (B4b), we expand σ^∞_{kn} as (29b) where only odd terms contribute. Furthermore, by making use of (A1d) and (30a)–(30d), we find

$$\begin{aligned}\boldsymbol{T}'_{D1} &= \varepsilon a\int_{Sp} 3\langle f\mathrm{S}_{1l}\rangle\mathrm{S}_{1l}\,\varepsilon_{imj}\,y_m\,\mathscr{C}\left(\delta_{jk} - n_j n_k\right)\\ &\quad\times\left[y_s\nabla_s\sigma^\infty_{kn}|_{\mathbf{x_p}} + \frac{y_p y_q y_r}{3!}\nabla_p\nabla_q\nabla_r\sigma^\infty_{kn}|_{\mathbf{x_p}} + \cdots\right] n_n\mathrm{d}S\\ &= -3\pi a^4\mathscr{C}\varepsilon\langle f\mathrm{S}_{1l}\rangle\varepsilon_{imj}\left[a\,\nabla_s\sigma^\infty_{kn}|_{\mathbf{xp}}\left(\frac{4}{15}A_{mnls}\delta_{jk} - \frac{4}{105}B_{mnjkls}\right)\right.\\ &\quad\left.+\frac{a^3}{6}\nabla_p\nabla_q\nabla_r\sigma^\infty_{kn}|_{\mathbf{x_p}}\left(\frac{4}{105}B_{mnpqrl}\delta_{jk} - \frac{4}{945}C_{mnpqrjkl}\right)\right]\\ &= -\frac{4}{5}\pi a^5\mathscr{C}\varepsilon\langle f\mathrm{S}_{1l}\rangle\varepsilon_{ijk}\nabla_j\sigma^\infty_{kl}|_{\mathbf{x_p}} - \frac{2}{35}\pi a^7\mathscr{C}\varepsilon\langle f\mathrm{S}_{1l}\rangle\varepsilon_{ijk}\nabla^2\nabla_j\sigma^\infty_{kl}|_{\mathbf{x_p}}\\ &= \frac{12}{5}\frac{\pi a^4}{(1+3\lambda)}\left(1 + \frac{a^2}{14}\nabla^2\right)\varepsilon_{ijk}\nabla_j\sigma^\infty_{kl}|_{\mathbf{x_p}}\varepsilon\langle f\mathrm{S}_{1l}\rangle. \end{aligned} \tag{B5}$$

For deriving Eq. (B5), we have used $\mathrm{S}_{1l} = -n_l$, $\varepsilon_{ijk}\sigma^\infty_{jk} = 0$ and $\nabla_j\sigma^\infty_{ij} = 0$.

$\boldsymbol{T}'_{D2}$ can be computed by using (A1b), (A1c), (30a), and (30b), giving

$$\begin{aligned}\boldsymbol{T}'_{D2} &= \varepsilon a\mu\int_{S_p} 3\langle f\mathrm{S}_{1_p}\rangle\mathrm{S}_{1p}\,\varepsilon_{ijk}y_j\,\mathscr{C}\delta_{kl}\,\mathscr{A}(\delta_{lm} - n_l n_m)(U_m - u^\infty_m(\mathbf{x_p}))\,\mathrm{d}S\\ &= -3\pi a^4\mathscr{A}\mathscr{C}\varepsilon\langle f\mathrm{S}_{1p}\rangle\varepsilon_{ijk}\left[\frac{4}{3}\delta_{pj}\delta_{km} - \frac{4}{15}A_{jpkm}\right](U_m - u^\infty_m(\mathbf{x_p}))\\ &= -\frac{18\pi a^4}{(1+3\lambda)^2}\,\varepsilon_{ijk}\,\varepsilon\langle f\mathrm{S}_{1j}\rangle(U_k - u^\infty_k(\mathbf{x_p})). \end{aligned} \tag{B6}$$

For deriving Eq. (B6), we have used $\delta_{jk}\varepsilon_{ijk} = 0$.

The end result can be obtained by combining (B5) and (B6), and written in terms of $\mathbf{P}_1 \equiv -\varepsilon\langle f\mathbf{S}_1\rangle$, giving (38).

b. Quadrupole torque T'_Q

The quadrupole torque $\boldsymbol{T}'_Q$ is also made of two contributions,

$$\boldsymbol{T}'_Q \equiv \boldsymbol{T}'_{Q1} + \boldsymbol{T}'_{Q2}, \tag{B7a}$$

$$\boldsymbol{T}'_{Q1} = \varepsilon a\int_{S_p} f(\mathbf{y})\,\varepsilon_{imj}y_m\,R^R_{jk||}\,\sigma^\infty_{kn}n_n\,\mathrm{d}S, \tag{B7b}$$

$$\boldsymbol{T}'_{Q2} = \varepsilon a\mu\int_{S_p} f(\mathbf{y})\,\varepsilon_{ijk}\,y_j\,R^R_{kl}\,R^R_{lm||}\,\varepsilon_{mpq}(\boldsymbol{\Omega}_p - \Omega^\infty_p(\mathbf{x_p}))y_q\,\mathrm{d}S. \tag{B7c}$$

$\boldsymbol{T}'_{Q1}$ is the torque exerted by the imposed flow stress, whereas $\boldsymbol{T}'_{Q2}$ is the torque arising from body rotation. To evaluate the former, we expand σ^∞_{kn} as (29b) where only even terms contribute. Using (A1b) and (30a)–(30d), we can evaluate (B7b) as

$$\begin{aligned}\boldsymbol{T}'_{Q1} &= a\int_{Sp}(5/6)\varepsilon\langle f\mathrm{S}_{2pq}\rangle\mathrm{S}_{2pq}\,\varepsilon_{imj}\,y_m\,\mathscr{C}\left(\delta_{jk} - n_j n_k\right)\\ &\quad\times\left[\sigma^\infty_{kn}(\mathbf{x_p}) + \frac{y_r y_s}{2!}\nabla_r\nabla_s\sigma^\infty_{kn}|_{\mathbf{x_p}} + \cdots\right] n_n\,\mathrm{d}S\\ &= \frac{5}{2}\pi a^4\mathscr{C}\varepsilon\langle f\mathrm{S}_{2pq}\rangle\varepsilon_{imj}\left[\sigma^\infty_{kn}(\mathbf{x_p})\left(\frac{4}{15}A_{pqmn}\delta_{jk} - \frac{4}{105}B_{pqmnjk}\right)\right.\\ &\quad\left.+\frac{a^2}{2}\nabla_r\nabla_s\sigma^\infty_{kn}|_{\mathbf{x_p}}\left(\frac{4}{105}B_{pqmnrs}\delta_{jk} - \frac{4}{945}C_{pqmnjkrs}\right)\right] \end{aligned}$$

$$= \frac{4}{3}\pi a^4 \mathscr{C}\, \varepsilon_{ipk}\, \varepsilon\langle f \mathrm{S}_{2pq}\rangle \left(1 + \frac{a^2}{14}\nabla^2\right) \sigma^{\infty}_{kq}(\mathbf{x_p}) + \frac{4}{21}\pi a^6 \mathscr{C}\, \varepsilon_{imk}\, \varepsilon\langle f \mathrm{S}_{2pq}\rangle\, \nabla_m \nabla_q\, \sigma^{\infty}_{kp}|_{\mathbf{x_p}}. \tag{B8}$$

For deriving Eq. (B8), we have used $\mathrm{S}_{2pq} = 3n_p n_q - \delta_{pq}$, $\varepsilon\langle f \mathrm{S}_{2pq}\rangle\delta_{pq} = 0$, and $\delta_{jm}\varepsilon_{imj} = 0$. Also notice that $\varepsilon_{ipk}\varepsilon\langle f \mathrm{S}_{2pq}\rangle\ \sigma^{\infty}_{kq} = \varepsilon_{ipk}\varepsilon\langle f \mathrm{S}_{2pq}\rangle 2\mu E^{\infty}_{kq}$ because $\varepsilon_{ipk}\varepsilon\langle f\, \mathrm{S}_{2pq}\rangle p^{\infty}\delta_{qk} = 0$. As a result, (B8) becomes

$$\boldsymbol{T}'_{Q1} = -\frac{8\pi\mu a^3}{(1+3\lambda)}\varepsilon_{ipk}\, \varepsilon\langle f \mathrm{S}_{2pq}\rangle \left(1 + \frac{a^2}{14}\nabla^2\right) E^{\infty}_{kq}(\mathbf{x_p}) - \frac{4}{7}\frac{\pi a^5}{1+3\lambda}\varepsilon_{imk}\, \varepsilon\langle f \mathrm{S}_{2pq}\rangle\, \nabla_m \nabla_q\, \sigma^{\infty}_{kp}|_{\mathbf{x_p}}. \tag{B9}$$

As for $\boldsymbol{T}'_{Q2}$ given by (B7c), we can compute it as follows using (A1c), (A1d), (30a), and (30b):

$$\begin{aligned}
\boldsymbol{T}'_{Q2} &= \varepsilon a(5/6)\mathscr{C}^2 \int_{Sp} \langle f \mathrm{S}_{2rs}\rangle (3n_r n_s - \delta_{rs}) \\
&\quad \times \varepsilon_{ijk}\, y_j\, \delta_{kl}(\delta_{lm} - n_l n_m)\varepsilon_{mpq}(\Omega_p - \Omega^{\infty}_p(\mathbf{x_p}))y_q\, \mathrm{d}S \\
&= \frac{5}{2}\pi a^5 \mathscr{C}^2 \varepsilon\langle f \mathrm{S}_{2rs}\rangle \varepsilon_{ijk}\varepsilon_{mpq}(\Omega_p - \Omega^{\infty}_p(\mathbf{x_p})) \\
&\quad \times \left(\frac{4}{15}A_{rsjq}\delta_{km} - \frac{4}{105}B_{rsjqkm}\right) \\
&= -\frac{4}{3}\pi a^5 \mathscr{C}^2 \varepsilon_{ijm}\varepsilon_{mpq}\,(\Omega_p - \Omega^{\infty}_p(\mathbf{x_p}))\, \varepsilon\langle f \mathrm{S}_{2jq}\rangle \\
&= -\frac{12\pi\mu a^2}{(1+3\lambda)}(\Omega_j - \Omega^{\infty}_j(\mathbf{x_p}))\, \varepsilon\langle f \mathrm{S}_{2ij}\rangle.
\end{aligned} \tag{B10}$$

For obtaining Eq. (B10), we have used $\varepsilon\langle f \mathrm{S}_{2pq}\rangle\delta_{pq} = 0$, $\varepsilon_{ijm}\varepsilon_{mpq} = \delta_{ip}\delta_{jq} - \delta_{iq}\delta_{jp}$, and $\delta_{mj}\varepsilon_{imj} = 0$.

Combining (B9) and (B10) gives (39) that is written in terms of $\mathbf{P}_2 \equiv \varepsilon\langle f \mathbf{S}_2\rangle$.

REFERENCES

[1] A. Walther and A. H. E. Muller, "Janus particles: Synthesis, self-assembly, physical properties, and applications," Chem. Rev. **113**, 5194–5261 (2013).

[2] S. Jiang, M. J. Schultz, Q. Chen, J. S. Moore, and S. Granick, "Solvent-free synthesis of Janus colloidal particles," Langmuir **24**, 10073–10077 (2008).

[3] P. Sundararajan, J. Wang, L. A. Rosen, A. Procopio, and K. Rosenberg, "Engineering polymeric Janus particles for drug delivery using microfluidic solvent dissolution approach," Chem. Eng. Sci. **178**, 199–210 (2018).

[4] T. J. Pedley, "Spherical squirmers: Models for swimming micro-organisms," IMA J. Appl. Math. **81**, 488–521 (2016).

[5] S. Wang and A. M. Ardekani, "Unsteady swimming of small organisms," J. Fluid Mech. **702**, 286–297 (2012).

[6] H. Nganguia, K. Zheng, Y. Chen, O. Pak, and L. Zhu, "A note on a swirling squirmer in a shear-thinning fluid," Phys. Fluids **32**, 111906 (2020).

[7] S. Yazdi and A. Borhan, "Effect of a planar interface on time-averaged locomotion of a spherical squirmer in a viscoelastic fluid," Phys. Fluids **29**, 093104 (2017).

[8] K. D. Housiadas, "An active body in a Phan-Thien and tanner fluid: The effect of the third polar squirming mode," Phys. Fluids **33**, 043110 (2021).

[9] A. Ramachandran and A. S. Khair, "The dynamics and rheology of a dilute suspension of hydrodynamically Janus spheres in a linear flow," J. Fluid Mech. **633**, 233 (2009).

[10] M. Trofa, G. D'Avino, and P. L. Maffettone, "Numerical simulations of a stick-slip spherical particle in Poiseuille flow," Phys. Fluids **31**, 083603 (2019).

[11] Q. Sun, E. Klaseboer, B. C. Khoo, and D. Y. C. Chan, "Stokesian dynamics of pill-shaped Janus particles with stick and slip boundary conditions," Phys. Rev. E **87**, 043009 (2013).

[12] A. R. Premlata and H. H. Wei, "The Basset problem with dynamic slip: Slip-induced memory effect and slip–stick transition," J. Fluid Mech. **866**, 431–449 (2019).

[13] A. R. Premlata and H.-H. Wei, "History hydrodynamic torque transitions in oscillatory spinning of stick–slip Janus particles," AIP Adv. **9**, 125113 (2019).

[14] J. Happel and H. Brenner, *Low Reynolds Number Hydrodynamics* (Prentice-Hall, 2012), Vol. 1.

[15] H. J. Keh and S. H. Chen, "The motion of a slip spherical particle in an arbitrary Stokes flow," Eur. J. Mech. B **15**, 791–807 (1996).

[16] A. R. Premlata and H. H. Wei, "Atypical non-Basset particle dynamics due to hydrodynamic slip," Phys. Fluids **32**, 097109 (2020).

[17] J. W. Swan and A. S. Khair, "On the hydrodynamics of 'slip–stick' spheres," J. Fluid Mech. **606**, 115–132 (2008).

[18] J. L. Anderson, "Effect of nonuniform zeta potential on particle movement in electric fields," J. Colloid Interface Sci. **105**, 45–54 (1985).

[19] J. Happel and H. Brenner, *Low Reynolds Number Hydrodynamics* (D. Reidel Publishing Co., Hingham, MA, 1983).

[20] H. Brenner, "The Stokes resistance of a slightly deformed sphere," Chem. Eng. Sci. **19**, 519–539 (1964).

[21] W. Zhang and H. A. Stone, "Oscillatory motions of circular disks and nearly spherical particles in viscous flows," J. Fluid Mech. **367**, 329–358 (1998).

[22] N. Oppenheimer, S. Navardi, and H. A. Stone, "Motion of a hot particle in viscous fluids," Phys. Rev. Fluids **1**, 014001 (2016).

[23] H. Masoud and H. A. Stone, "The reciprocal theorem in fluid dynamics and transport phenomena," J. Fluid Mech. **879**, P1 (2019).

[24] H. Brenner, "The Stokes resistance of an arbitrary particle-II: An extension," Chem. Eng. Sci. **19**, 599–629 (1964).

[25] K. Kamrin and H. A. Stone, "The symmetry of mobility laws for viscous flow along arbitrarily patterned surfaces," Phys. Fluids **23**, 031701 (2011).

[26] C. P. Martin, S. Wang, and S. Kim, "Surface tractions on an ellipsoid in Stokes flow: Quadratic ambient fields," Phys. Fluids **31**, 021209 (2019).

[27] G. Batchelor, "The stress system in a suspension of force-free particles," J. Fluid Mech. **41**, 545–570 (1970).